

DEVELOPMENT OF WHOLE CELL BIOREPORTERS FOR DETECTION OF
BORIC ACID, CYANIDE AND PARAQUAT

A THESIS SUBMITTED TO
THE GRADUATE SCHOOL OF NATURAL AND APPLIED SCIENCES
OF
MIDDLE EAST TECHNICAL UNIVERSITY

BY

MELEK SULUOVA

IN PARTIAL FULFILLMENT OF THE REQUIREMENTS
FOR
THE DEGREE OF MASTER OF SCIENCE
IN
MOLECULAR BIOLOGY AND GENETICS

SEPTEMBER 2019

Approval of the thesis:

**DEVELOPMENT OF WHOLE CELL BIOREPORTERS FOR DETECTION
OF BORIC ACID, CYANIDE AND PARAQUAT**

submitted by **MELEK SULUOVA** in partial fulfillment of the requirements for the degree of **Master of Science in Molecular Biology and Genetics Department, Middle East Technical University** by,

Prof. Dr. Halil Kalıpçılar
Dean, Graduate School of **Natural and Applied Sciences**

Prof. Dr. Ayşe Gül Gözen
Head of Department, **Molecular Biology and Genetics**

Prof. Dr. Hüseyin Avni Öktem
Supervisor, **Molecular Biology and Genetics, METU**

Examining Committee Members:

Prof. Dr. Füsün İnci Eyidoğan
Education Faculty, Başkent University

Prof. Dr. Hüseyin Avni Öktem
Molecular Biology and Genetics, METU

Prof. Dr. Ayşen Tezcaner
Engineering Science, METU

Date: 13.09.2019

I hereby declare that all information in this document has been obtained and presented in accordance with academic rules and ethical conduct. I also declare that, as required by these rules and conduct, I have fully cited and referenced all material and results that are not original to this work.

Name, Surname: Melek Suluova

Signature:

ABSTRACT

DEVELOPMENT OF WHOLE CELL BIOREPORTERS FOR DETECTION OF BORIC ACID, CYANIDE AND PARAQUAT

Suluova, Melek
Master of Science, Molecular Biology and Genetics
Supervisor: Prof. Dr. Hüseyin Avni Öktem

September 2019, 73 pages

Chemical industry is one of the fastest growing sectors in the world due to immensely increasing human population. In despite of precautions ruled by legislations, many chemicals are produced and released to into environment. These pollutants get into soil, water and air thus to our food, resulting in serious toxic effects on human health and the destruction of ecosystems.

Boric acid, paraquat and cyanide are example for pollution causing chemicals. Due to their possible toxicity, continuous monitoring is needed on environmental samples.

Whole cell biosensors are one of the promising devices to screen various compounds in environmental samples. They are analytical devices that convert a biological response into an electrical signal. These systems have a lot of advantageous properties in comparison with chemical methods.

The aim of this study was to develop whole cell biosensor method by designing new bioreporter cell constructs against boric acid, cyanide and paraquat. *E. coli* K12 MG1655 was used as a model organism and green fluorescence protein gene (*gfp*) was used as a reporter gene. By this study, *grpE* gene promoter was used for the first time for the detection of boric acid. It was detected at 18th hour with 50 mM detection limit.

hdeBAD operon promoter included in cyanide detection in this study was not used before in bioreporter studies at all. By using this promoter, cyanide was detected at 3rd hour with 100 μ M detection limit. *sodA* gene promoter is widely used for paraquat detection studies. In this work, lower detection range was tested. Therefore, paraquat was detected at 18th hour with 50 nM detection limit. At least 400% increase in fluorescence signal was observed in the experimental groups compared to the control group for detection of all three chemicals.

Three different bioreporter cell groups developed in this study can be further developed and used in the production of fast, easy to use and on-site measurement systems.

Keywords: Boric Acid, Paraquat, Cyanide, Whole Cell Biosensor, Bioreporter

ÖZ

BORİK ASİD, SİYANÜR VE PARAKUAT TESPİTİ İÇİN HÜCRE ESASLI BİYORAPORTÖRLERİN GELİŞTİRİLMESİ

Suluova, Melek
Yüksek Lisans, Moleküler Biyoloji ve Genetik
Tez Danışmanı: Prof. Dr. Hüseyin Avni Öktem

Eylül 2019, 73 sayfa

Kimya endüstrisi, hızla artan insan nüfusu nedeniyle dünyanın en hızlı büyüyen sektörlerinden biridir. Yasaların öngördüğü önlemlere rağmen, birçok kimyasal üretilir ve çevreye bırakılır. Bu kirletici maddeler toprağa, suya, havaya ve de besinlerimize karışarak, sahip oldukları ciddi toksik etkiler sebebiyle insan sağlığının ve ekosistemlerin tahrip edilmesine neden olmaktadır.

Borik asit, paraquat ve siyanür, kirliliğe neden olan kimyasallara örneklerdir. Olası toksisiteleri nedeniyle çevresel numunelerde sürekli takip edilmeleri gerekir.

Hücre esaslı biyosensörler, çevresel numunelerdeki çeşitli bileşikleri taramak için gelecek vadeden cihazlardan biridir. Biyolojik bir cevabı elektrik sinyaline dönüştüren analitik cihazlardır. Bu sistemler, kimyasal yöntemlerle karşılaştırıldığında birçok avantajlı özelliğe sahiptir.

Bu çalışmanın amacı, borik asit, siyanür ve parakuata karşı yeni biyoreportör hücre yapıları tasarlayarak hücre esaslı biyosensör yöntemini geliştirmektir. Model organizma olarak *E. coli* K12 MG1655, raportör gen olarak da yeşil floresan protein geni (*gfp*) kullanıldı. Bu çalışmayla, *grpE* gen promotörü ilk kez borik asit tespitinde kullanıldı. Borik asit, 18. saatte 50 mM saptama limiti ile tespit edildi. Bu çalışmada siyanür tespitinde kullanılan *hdeBAD* operon promotörü daha önce hiç biyoreportör

çalışmalarında kullanılmamıştır. Bu promotör kullanılarak, siyanür 3. saatte 100 uM saptama limiti ile tespit edildi. *sodA* gen promotörü, paraquat tespiti için yapılan çalışmalarda yaygın olarak kullanılmaktadır. Bu çalışmada, düşük konsantrasyon aralığı test edildi. Sonuç olarak paraquat 18. saatte 50 nM algılama sınırı ile tespit edildi. Üç kimyasalın tespitinde de kontrol grubuna göre deney gruplarında en az %400'lük bir floresan sinyal artışı gözlemlendi.

Bu çalışmada geliştirilen üç farklı biyoreportör hücre grubu daha da geliştirilerek, hızlı, kullanımı kolay, sahadan ölçüm imkânı veren sistemlerin üretilmesinde kullanılabilir.

Anahtar Kelimeler: Borik Asit, Parakuat, Siyanür, Hücre Esaslı Biyosensör, Biyoreportör

To My Family...

ACKNOWLEDGEMENTS

I would like to express my special thanks of gratitude to my supervisor Prof. Dr. Hüseyin Avni ÖKTEM for his valuable guidance, encouragement, patience and kindness throughout this study.

I am also grateful to Evrim Elçin for her endless support, patience and mentorship. Owing to her contributions and help, I was motivated to carry out and complete this study.

I would like to thank to examining committee members Prof. Dr. Ayşen TEZCANER and Prof. Dr. Füsün İnci EYİDOĞAN for their involvement, evaluation and kind feedback.

I am also thankful to all members of ÖKTEM Lab family for their endless technical and emotional support, precious comments and friendships.

My biggest genuine gratefulness belongs to my parents Süsanber & Aydın Coşkunsu, my brother Tolga Coşkunsu and my dear husband Sefa Suluova. Without their endless love and support throughout my life, I would not be able to complete this thesis.

This study was supported by Middle East Technical University/ Scientific Research Project Coordination Office (METU-BAP), Project No: BAP/ YLT:108-2018-3533 and Scientific and Technical Research Council of Turkey (TÜBİTAK) 2522-TÜBİTAK (Turkey) - NRDIO (Hungary) Joint Funding Program; Project No: 217E115.

I would like to thank Scientific and Technical Research Council of Turkey (TÜBİTAK) for their 2210-C National MSc/MA Scholarship Program in the Primary Fields in Science and Technology.

TABLE OF CONTENTS

ABSTRACT	v
ÖZ	vii
ACKNOWLEDGEMENTS	x
TABLE OF CONTENTS	xi
LIST OF TABLES	xv
LIST OF FIGURES	xvii
LIST OF ABBREVIATIONS	xix
CHAPTERS	1
1. INTRODUCTION	1
1.1. Environmental Pollution.....	1
1.1.1. Classification of Environmental Pollutants	1
1.1.1.1. Pesticide	2
1.1.1.2. Paraquat and H ₃ BO ₃	3
1.1.1.2.1. Paraquat	3
1.1.1.2.2. H ₃ BO ₃ as Pesticide Component	4
1.1.1.3. Cyanide	5
1.2. Detection Methods	7
1.2.1. Paraquat Detection Methods.....	7
1.2.2. H ₃ BO ₃ Detection Methods.....	8
1.2.3. Cyanide Detection Methods.....	8
1.3. Whole Cell Biosensor.....	9
1.3.1. Principle of Bioreporter	11

1.3.2. Classification of Bioreporters	12
1.3.2.1. Cell Types	12
1.3.2.2. Promoters	13
1.3.2.2.1. Heat Shock Gene Promoter, <i>grpE</i>	13
1.3.2.2.2. <i>hdeBAD</i> Operon Promoter	14
1.3.2.2.3. <i>sodA</i> Gene Promoter	14
1.3.2.3. Reporter Genes	15
1.3.2.4. Detection Methods	16
1.4. Aim of the Study	16
2. MATERIALS & METHODS	19
2.1. MATERIALS	19
2.1.1. Chemicals and Enzymes	19
2.1.2. Media and Kits	19
2.1.3. Buffers and Solutions	19
2.1.4. Bacterial Strains, Plasmids and Primers	20
2.1.5. Instruments	21
2.2. METHODS	22
2.2.1. Growth Conditions of Bacteria Strains	22
2.2.2. Preparation of Competent Bacteria	22
2.2.3. Agarose Gel Electrophoresis	23
2.2.4. Molecular Genetics Methods	23
2.2.4.1. Genomic DNA Isolation from <i>E. coli</i> K-12 MG1655 Cells	23
2.2.4.2. Polymerase Chain Reaction (PCR) Primer Design of <i>hdeB</i> Gene Promoter from gDNA of <i>E. coli</i> K-12 MG1655 Cells	24

2.2.4.3. Amplification of Promoters.....	24
2.2.4.3.1. Gradient PCR	24
2.2.4.3.2. Phusion (High Fidelity) PCR	26
2.2.4.4. Purification of PCR Products	26
2.2.4.5. pBR-sGFP Plasmid Isolation from Transformed <i>E. coli</i> K-12 DH5 α Cells	27
2.2.4.6. Restriction Digestion for Insert and Vector Preparation.....	27
2.2.4.7. Purification of Restriction Digestion Products	28
2.2.4.8. Ligation Reaction	28
2.2.4.9. Transformation of Competent <i>E. coli</i> K-12 DH5 α Cells	29
2.2.4.10. Colony PCR	29
2.2.4.11. Plasmid Isolation from Transformed <i>E. coli</i> K-12 DH5 α Cells.....	31
2.2.4.12. Restriction Cut of Plasmid for Verification	31
2.2.4.13. Transformation of Competent <i>E. coli</i> K-12 MG1655 Cells.....	32
2.2.4.14. Plasmid Isolation from Transformed <i>E. coli</i> K-12 MG1655 Cells ..	32
2.2.5. Induction Assays.....	33
2.2.5.1. H ₃ BO ₃ (Boric Acid) Detection by <i>grpE</i> Gene Promoter	33
2.2.5.2. KCN (Cyanide) Detection by <i>hdeB</i> Gene Promoter	34
2.2.5.3. Paraquat Detection by <i>sodA</i> Gene Promoter	34
2.2.5.4. Fluorescence Measurement	35
2.2.5.5. Microscope Image	36
2.2.5.6. Data Analysis	36
3. RESULTS & DISCUSSION	37
3.1. Cloning Studies with <i>E. coli</i> Cells.....	37

3.1.1. Genomic DNA Isolation from <i>E. coli</i> K-12 MG1655 Cells.....	37
3.1.1.1. Gradient PCR to Decide Annealing Temperature of Primers	39
3.1.1.2. Cloning of <i>hdeB</i> Gene Promoter into pBR-sGFP Plasmid.....	40
3.1.2. Restriction Digestion for Insert and Vector Preparation and Purification	41
3.1.3. Colony PCR from Transformed <i>E. coli</i> K-12 DH5 α Cells	43
3.1.4. Conformation of Ligation.....	44
3.2. Induction Assays	46
3.2.1. H ₃ BO ₃ Detection	46
3.2.2. KCN (Cyanide) Detection	50
3.2.3. Paraquat Detection	54
4. CONCLUSION	59
REFERENCES	61
APPENDICES	65
A. BACTERIAL GROWTH MEDIA	65
B. BUFFERS AND SOLUTIONS	67
C. <i>hdeBAD</i> OPERON DNA SEQUENCE	69
D. EXAMPLES FOR RFU RESULTS OF INDUCTION GROUPS.....	71

LIST OF TABLES

TABLES

Table 1.1 Examples from commonly used reporter genes	15
Table 2.1 Primer sequences for amplification of <i>hdeB</i> gene promoter	24
Table 2.2 Gradient PCR reaction mixture	25
Table 2.3 Gradient PCR reaction condition for 465bp amplicon	25
Table 2.4 Phusion PCR reaction mixture	26
Table 2.5 Phusion PCR reaction condition for 465 bp amplicon	26
Table 2.6 Restriction digestion reaction	28
Table 2.7 Ligation reaction mixture	28
Table 2.8 Colony PCR reaction mixture	30
Table 2.9 Colony PCR primer regions	30
Table 2.10 Conditions of colony PCR.....	30
Table 2.11 Restriction cut reaction.....	31
Table 2.12 H ₃ BO ₃ detection by <i>grpE</i> gene promoter	34
Table 2.13 KCN (cyanide) detection by <i>hdeB</i> gene promoter	34
Table 2.14 Paraquat detection by <i>sodA</i> gene promoter	35
Table 3.1 Purity of MG1655 gDNA.....	37
Table 3.2 Absorbance values of pBR322 and seven pBR- <i>grpE</i> -sGFP induction groups at distinct time points	46
Table 3.3 RFU values of boric acid treated seven pBR- <i>grpE</i> -sGFP induction groups at distinct time points	47
Table 3.4 Absorbance values of pBR322 and seven pBR- <i>hdeB</i> -sGFP induction groups at distinct time points	50
Table 3.5 RFU values of potassium cyanide treated seven pBR- <i>hdeB</i> -sGFP induction groups at distinct time points	52

Table 3.6 Absorbance values of pBR322 and six pBR- <i>sodA</i> -sGFP induction groups at distinct time points.....	54
Table 3.7 RFU values of paraquat treated six pBR- <i>grpE</i> -sGFP induction groups at distinct time points.....	56

LIST OF FIGURES

FIGURES

Figure 1.1 Chemical structure of paraquat	4
Figure 1.2 On/off switch systems of bioreporters	11
Figure 1.3 Examples for different detection methods	16
Figure 2.1 pBR-sGFP Map.....	21
Figure 3.1 1% Agarose Gel Electrophoresis Result for <i>E. coli</i> MG1655 gDNA.....	38
Figure 3.2 1% Agarose gel electrophoresis for PCR products.....	39
Figure 3.3 1% Agarose gel electrophoresis result for pBR-sGFP plasmid and Phusion PCR products.	40
Figure 3.4 1% Agarose gel electrophoresis result for purified restriction digestion products.....	42
Figure 3.5 1% Agarose gel electrophoresis result for colony PCR products.....	43
Figure 3.6 1% Agarose gel electrophoresis result for conformation of ligation.	44
Figure 3.7 1% Agarose gel electrophoresis result for conformation of <i>E. coli</i> K-12 MG1655 cells transformation.	45
Figure 3.8 Growth curves of pBR322 and boric acid treated seven pBR- <i>grpE</i> -sGFP induction groups at distinct time points	47
Figure 3.9 % increase of fluorescence (RFU) for six boric acid treated groups in comparison with control group at distinct time points.....	48
Figure 3.10 Fluorescence microscope images of control group and 50 mM H ₃ BO ₃ treated induction group at 18th hour	49
Figure 3.11 Growth curves of pBR322 and cyanide treated seven pBR- <i>hdeB</i> -sGFP induction groups at distinct time points	51
Figure 3.12 % increase of fluorescence (RFU) for six cyanide treated groups in comparison with control group at distinct time points.....	53

Figure 3.13 Fluorescence microscope images of control group and 100 μ M KCN treated induction group at 3rd hour	53
Figure 3.14 Growth curves of pBR322 and paraquat treated six pBR- <i>sodA</i> -sGFP induction groups at distinct time points.....	55
Figure 3.15 % increase of fluorescence (RFU) for five paraquat treated groups in comparison with control group at distinct time points	57
Figure 3.16 Fluorescence microscope images of control group and induced group with 1 μ M paraquat at 18th hour	57
Figure A.1 Amplified region of hdeBAD operon promoter	69
Figure A.2 RFU value of 40 mM H ₃ BO ₃ induced sample at 9 th hour	71
Figure A.3 RFU value of 100 μ M KCN induced group at 9th hour.....	72
Figure A.4 RFU value of 2.5 μ M paraquat induced group at 9 th hour	73

LIST OF ABBREVIATIONS

ABBREVIATIONS

dH₂O: Distilled water

DNA: Deoxyribonucleic acid

dNTP: Deoxyribonucleotide triphosphate

gDNA: Genomic DNA

kb: Kilobase

LB: Luria-Bertani

mL: Milliliter

mM: Millimolar

nm: Nanometer

PAH: Polycyclic aromatic hydrocarbon

PBS: Phosphate buffered saline

PCR: Polymerase chain reaction

PM: Particulate matter

RbCl: Rubidium chloride

RFU: Relative fluorescence unit

ROS: Reactive oxygen species

T_m: Primer melting temperature

um: Micrometer

V: Volt

CHAPTER 1

INTRODUCTION

1.1. Environmental Pollution

Chemical industry is one of the fastest growing sectors in the world due to immensely increasing human population. Most popular areas are pharmaceuticals, agrochemicals, paints, plastic, rubber, coating and widely produced almost all over the world including US, Canada, Latin America, Europe and the Asia-pacific (J. H. Lee, Youn, Kim, & Gu, 2007). In despite of precautions ruled by legislations, many chemicals are produced and released to into environment. In addition to this, household activities, transport, energy production and waste management are different ways causing environmental pollution. These pollutants get into soil, water, air, and finally to our food, resulting in serious toxic effects on human health and destruction of the ecosystems (Konduracka, 2019).

Today, despite of increased awareness and developed medical care not only low- or middle-income countries but also high-income ones suffer from health effects of pollutants. Thus, toxicity of environmental pollutants should be assessed properly and their release into the environment should be tracked carefully.

1.1.1. Classification of Environmental Pollutants

There are a lot of potentially harmful chemicals, the most common ones include particulate matter (PM) pollutants, nitrogen oxides, polycyclic aromatic hydrocarbons (PAHs), heavy metals, pesticides, hormones, and pharmaceuticals. Exposition to these chemicals can cause skin irritation, and affect respiratory and digestion systems (Konduracka, 2019).

As an example, pharmaceutical release to the environment (air, soil and water) is one of the reasons of pollution. In addition to pharmaceuticals, their transformation products become a global concern because of steady increase in human population and pharmaceutical formulations. Moreover, some of the pharmaceuticals may have long half-life so they can accumulate in the environment. Based on various assessments, approximately 160 pharmaceuticals in soil, wastewater and ground water were recorded and some active components were detected in drinking water (Parezanović et al., 2019).

1.1.1.1. Pesticide

Pesticides are chemical compounds that are used for destroying or repelling pests like insects, rodents, fungi, or weeds. Most of the time, toxic action mechanism of pesticides is not specific to target so this affects ecosystem and biodiversity negatively. Killing of bees, amphibians, birds, fish and small mammals are recorded due to this reason (Carvalho, 2017). Excessive usage of pests due to high demand on food production is the biggest reason for accumulation of agrochemicals in the environment. Today, exposure to pesticides is inevitable and these chemicals are accepted as cause of many diseases such as cancer, obesity, endocrine disruptions and other diseases in humans. Recently a study has shown a positive correlation between pesticide concentration and cardio-vascular disease among farmworkers (Konduracka, 2019). Moreover, due to excessive and inappropriate usage of pesticide, death of approximately 355,000 people is recorded every year (Carvalho, 2017).

Pesticides can be classified based on their targets. Major classes consist of insecticides, herbicides, fungicides and rodenticides. Further classification can be done based on chemical content, physical state, application method and origin of derivation (Richardson, Fitsanakis, Westerink, & Kanthasamy, 2019). Common chemical groups included in pesticides are organochlorine, organophosphate,

carbamate, pyrethroids, growth regulators (for crops), neonicotinoids, and lately developed biopesticides (Carvalho, 2017).

Human population has climbed up from 1.5 billion to 6.1 billion between 1900 and 2000 years, and estimated world population has expected to be 9.4-10 billion by 2050. Therefore, to deal with immense growth in population, agricultural production increased immensely. To increase crop yield and food production, pesticide and agrochemical usage became an obligation. However, their excessive usage caused significant contamination of terrestrial ecosystems and poisoning human foods (Carvalho, 2017).

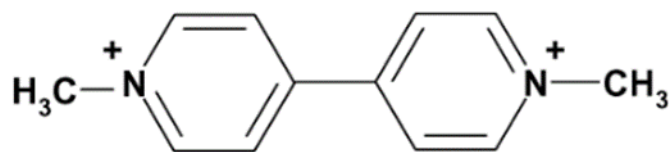
Today, approximately 3.6 billion kg active ingredient is used as pesticide in the world per year (Richardson et al., 2019).

1.1.1.2. Paraquat and H₃BO₃

1.1.1.2.1. Paraquat

Paraquat was used as oxidation and reduction indicator before discovery of herbicidal properties. Due to violet/blue color of free radical monocation form (PQ⁺), paraquat is commonly known as methyl viologen. It was firstly introduced into the agricultural market in 1950s. Today, more than 120 developed and developing countries are using paraquat as herbicide despite of numerous intoxications (Dinis & Oliveira, 2008).

Paraquat, N, N'-dimethyl-4,4'-bipyridinium dichloride, is a none-selective and highly efficient herbicide. Poisoning cases mostly end up with death due to lack of selective antidote. Multiple organ damage is observed. Bronchial and alveolar injury in lungs gives rise to acute respiratory syndrome which is the most frequent cause of paraquat fatality (Moloudizargari et al., 2019).



PQ (1,1'-dimethyl-4,4'-bipyridylium ion)

Figure 1.1 Chemical structure of paraquat (Dinis & Oliveira, 2008)

After agricultural applications of paraquat, it is absorbed by soil and transported to water due to high water solubility and low volatility. Thus, natural water sources can easily be contaminated by excessive and inappropriate paraquat usage. In addition to terrestrial systems, aquatic organisms like algae, crayfish, insects and fish are affected by toxicity of paraquat (Chuntib & Jakmune, 2015).

1.1.1.2.2. H_3BO_3 as Pesticide Component

Boron is an inorganic compound naturally found in soils and rocks. Multiple boron compounds such as boric acid, boron oxide, borate salts like sodium tetraborate, disodium octaborate and sodium metaborate are found in the environment in combination with oxygen (Aguilera-Sáez et al., 2018). Due to their biocidal feature, boron compounds are used in production of detergents, cleaners, personal care products, glass, ceramic, agriculture products like fertilizers and also biocides (Schoderboeck et al., 2011). Moreover, 8% and higher concentration of boric acid is found to have an effect as fungicide for protection of vegetables and fruit trees. It is also used in insecticide and herbicide production for agricultural and non-food purposes (Aguilera-Sáez et al., 2018; Hamilton & Wolf, 2007).

Prevalent usage of boron compounds and its high solubility in waters raise concern about its possible toxicity. Since boron content in all discarded product will be end up

in water so accumulation can cause problem. Therefore, European Chemicals Agency classified boric acid as a high concern substance for being toxic for reproduction in 2010. That means it can cause fertility problems and give harm to unborn child (Princz et al., 2017). After that, boron concentration in any kind of product is restricted to less than 1% in European countries (Schoderboeck et al., 2011).

Dose-dependent boron treatment studies on animals like rats, mice and dogs resulted in testicular toxicity by symptoms like lower spermiation and decrease in epididymal sperm counts. However, several field studies that are conducted by participation of males from boron rich areas (mainly from boron producing factory workers) with 9.5 mg/L and 29 mg/L boron concentrations in drinking water in Turkey showed no adverse of boron exposure on male reproductive system. Similar studies in China showed similar results (Taylor & Bolt, 2014). Even boron compounds and boric acid do not show any impairment in reproduction system, accumulation of boric acid in the environment will continue to give harm other organisms. Thus might disrupt the ecosystems. So continuous measurement of boric acid from environmental samples is crucial.

1.1.1.3. Cyanide

Cyanide compounds contain $C\equiv N$ group, named as cyano group. They are available in different forms such as nitriles, carbonitriles and cyanides. Various sources contribute the presence of cyanides in nature. Plants, fungi, microorganism, especially bacteria release cyanide to environment via a mechanism called as “cyanogenesis”. In addition to natural activities, human activities also cause increase of cyanide level in nature. Compounds that contain cyano group are used in different areas in industry like pharmaceutical, polymer manufacturing, electroplating, mining and agricultural production. Especially mining and agricultural purposes have high effect in increase of environmental cyanide amount. In metal mining process, cyanide is used to help extraction of gold, silver, iron and heavy metals from ore by forming tight complexes.

Agricultural practices are another cause for increase in cyanide amount in soil, water and environment. Nitrile containing herbicides like dichlorobenil, ioxynil, bromoxynil and chlorothalonil are examples used for controlling pest in crop production (Sharma, Akhter, & Chatterjee, 2019).

Cyanide ions (CN^-) are extremely toxic for living organisms and humans. It binds strongly to Fe^{3+} of heme cofactors in cytochrome C oxidase and inhibits its oxygen transport function. Thus, paralysis in cellular respiration is observed in addition to serious damage in central nervous system. Accidental high amount of cyanide intake causes rapid death in humans. The oral lethal dose is estimated as 1.4 mg kg^{-1} body weight for humans (Dong et al., 2017; Zhang et al., 2015). Antidotes for cyanide intoxication are prepared as kit that contains amyl nitrite, sodium nitrite and sodium thiosulphate which binds to mitochondrial enzyme rhodanese and facilitates cyanide conversion to thiocyanate. Hydroxocobalamin is a newer antidote, acts by binding cyanide and forms cyanocobalamin (Jethava, Gupta, Kothari, Rijhwani, & Kumar, 2014).

During industrial practices, unintentional cyanide release may happen to nature. According to studies, continuous cyanide leakage to waters negatively affect swimming and fish reproduction in concentrations between $5.0 \mu\text{gL}^{-1}$ (190 nM) and $7.2 \mu\text{gL}^{-1}$ (280 nM). Concentrations higher than $6.1 \mu\text{M}$ can cause acute health problems in many freshwater species from fishes to invertebrates. Permitted cyanide level of CN^- in drinking water is determined as $2.7 \mu\text{M}$ by World Health Organization (WHO) (Lien et al., 2018).

1.2. Detection Methods

1.2.1. Paraquat Detection Methods

Due to its toxic nature, paraquat concentration in nature should be followed carefully. Various assays for paraquat detection are available. They are flow injection colorimetric assays, fluorescent probe titration, gas chromatography-mass spectrometry, radioimmunoassay and spectrophotometry. Common disadvantages of these method are the need for complex instrumentation and lab-based measurements. Recently, electrochemical approach was applied for paraquat detection. Less expensive, simple and easy to use instruments are developed for this approach.

According to several studies about electrochemical detection of paraquat, the system is based either on bare or copper electrodes, electrodes modified with metal nanoparticles, carbon nanomaterials, organic and polymeric compounds and inorganic materials. On site application of these methods is applicable. Moreover, detection limit by these systems is below the internationally permissible limit of paraquat in drinking water. Solid support like mesoporous silica thin films strengthen electrochemical detection of cationic paraquat in water samples (Nasir et al., 2018)

Chromatography is a commonly used technique among the analytical methods for paraquat detection in various samples. In spite of high sensitivity and multi-analytes capability, time consuming cleaning steps and complex instrumentation affect the preference of this method. On the other hand, voltammetric methods do not require pre-treatments, so enable fast result. Mechanism of action is based on redox reaction and the peak of current is directly proportional to paraquat concentration in samples. Another widely used approach for paraquat screening is spectrophotometric method. Reducing agents like sodium dithionite, sodium borohydride and dehydroascorbic acid are used for reduction of paraquat in an alkaline medium. As a result, produced blue free radical ions are measured by spectrophotometer. Since blue product is not stable, method is not convenient for batchwise applications. Finally, more recent method flow injection analysis system combines spectrophotometric and

voltammetric approaches. This system enables improved sensitivity, and saves on chemicals and time (Chuntib & Jakmune, 2015).

1.2.2. H₃BO₃ Detection Methods

Analytic measurement of boric acid can be done by several methods including spectrophotometric methods, acid-base titrations, potentiometric titrations, ion and gas chromatography and inductively coupled plasma mass spectrometry (ICP-MS). Most of these methods require sophisticated instrumentation, pre-treatments or dilution steps if sample concentration is too high. Thus, these make these methods expensive and time-consuming. Recently, a quantitative boron-11 NMR method was developed to determine the boric acid concentration in commercial biocide. It enables simple sample preparation and direct measurements without complex dilution steps (Aguilera-Sáez et al., 2018).

1.2.3. Cyanide Detection Methods

Due to its toxic nature for organisms and extensive usage in industry, cyanide should be followed carefully in environment. Common cyanide detection methods are chromatography, potentiometry and conventional titrations, voltammetric and electrochemical techniques (Zhang et al., 2015). However, these systems are expensive and time consuming as they require complex instrumentation and skillful analysts. In addition to these methods, colorimetric and fluorometric approaches are developed by using dyes and nanomaterials to eliminate disadvantages and improve selectivity, sensitivity and simplicity of cyanide detection systems (Lien et al., 2018).

Gold (Au) or silver (Ag) nanoparticles are widely used for cyanide sensing in colorimetric systems. In the presence of oxygen Au/Ag-CN complexes are formed. These nanoparticles are also used in fluorescent probes that have higher sensitivity than colorimetric methods. Lately, a new nanoparticle, bimetallic core-shell NP has

been developed and reported that it exhibited high simplicity, sensitivity, selectivity and rapidity for cyanide ion detection (Dong et al., 2017).

Fluorescent chemosensor is another system which offers similar features. Additionally, it enables visual detection, optical imaging, on-site and real time detections. Some of the organic fluorescent probes include various electron deficient functional groups. Since the action mechanism of the system is based on the reaction of cyanide with these chemicals such as oxazine, pyrylium, acridinium, imidazole, salicylaldehyde and others. However, these kind of probes need to be used in organic solvent containing media and have low sensitivity in water (Promchat, Rashatasakhon, & Sukwattanasinitt, 2017).

1.3. Whole Cell Biosensor

Biosensor is an analytical device that measures target chemical in the sample by combining biological components with a physiochemical detector. Biological part of the sensor can be DNA, enzyme, protein or whole cell. Whole cell biosensors are considerably useful to get information about cell biology, toxicology, pharmacology and environmental measurements. In some of water quality assays, aqueous animals such as fish and shrimp are included. This requires detailed procedure, high cost and long time (Wasito, Fatoni, Hermawan, & Sutji, 2019). Instead of benefiting from multicellular organism in environmental measurements, preparing biosensor by the help of microorganism has more advantages. Microorganisms have short life span and give fast response to pollution and toxins. Due to their ability to adapt extreme conditions and stress responsive traits, microorganisms are good candidates to be used in whole cell biosensors for toxicity detection in environmental studies (Zhai et al., 2013).

Microorganisms are convenient model organisms for genetic studies. Researchers have unlimited opportunity to combine sensory and reporter genes to adjust sensitivity, speed and specificity. For example, most of the bioreporters respond more

than one target so it is difficult to detect presence of specific target. By the help of genetic manipulation techniques, modifications can be applied for improvements of specificity. One of the important advantages of biosensors is the ability to report on bioavailability which gives ratio of chemical that freely pass the cell membrane and has biological effect on it. Therefore, rather than total concentration, it gives information about effects on organisms (Xu et al., 2013).

After genetic modifications applied on cells for sensory purposes, immobilization technique is applied to be able to use them without losing their bioreceptor ability. Trapping method is the most common among immobilization techniques. Cells are trapped in a solid matrix polymer that can compose of agarose, acrylamide, chitosan and alginate. The last one is more advantageous than others by having good biocompatibility and low toxicity (Wasito et al., 2019).

Whole cell biosensor method has plenty of advantages when it is compared with chemical analysis approaches. It can reveal potential synergistic/antagonistic effects between multiple pollutants, give insight about bioavailability, offer better estimate of the real toxicology potential of the sample. Moreover, since it does not require sophisticated instrumentation and a lot of expertise, so it is easy to perform, time saving and less expensive than standard methods.

In general, whole cell biosensor can give first insight about presence or absence of target chemical or pollution. Therefore, it should be mentioned that bioreporter usage does not fully aim to replace chemical analytical methods. Instead, bioreporter cells and chemical analytical approaches can be combined for environmental assessments. Taking samples from large areas periodically and using sophisticated methods cause loss of money and time. Moreover, most of the time, samples are labeled as below the safety limit. So, bioreporter assays can provide on-site information about the pollution and when strong signal is obtained from the site, more precise approach will be followed (Xu et al., 2013).

1.3.1. Principle of Bioreporter

Bioreporters are living sensors which can be composed of prokaryotic (bacteria) or eukaryotic (algae, fungi, animal) cells. By the help of evolution, they contain some specific features to deal with toxicity of various environments. Thus, they have mechanisms to adapt and defense against chemicals. Due to these features, by using genetic engineering techniques and synthetic biology tools, they can be converted to controllable on/off switch systems. There are two types of systems as lights-on and lights-off (Xu et al., 2013) as illustrated at Figure 1.2.

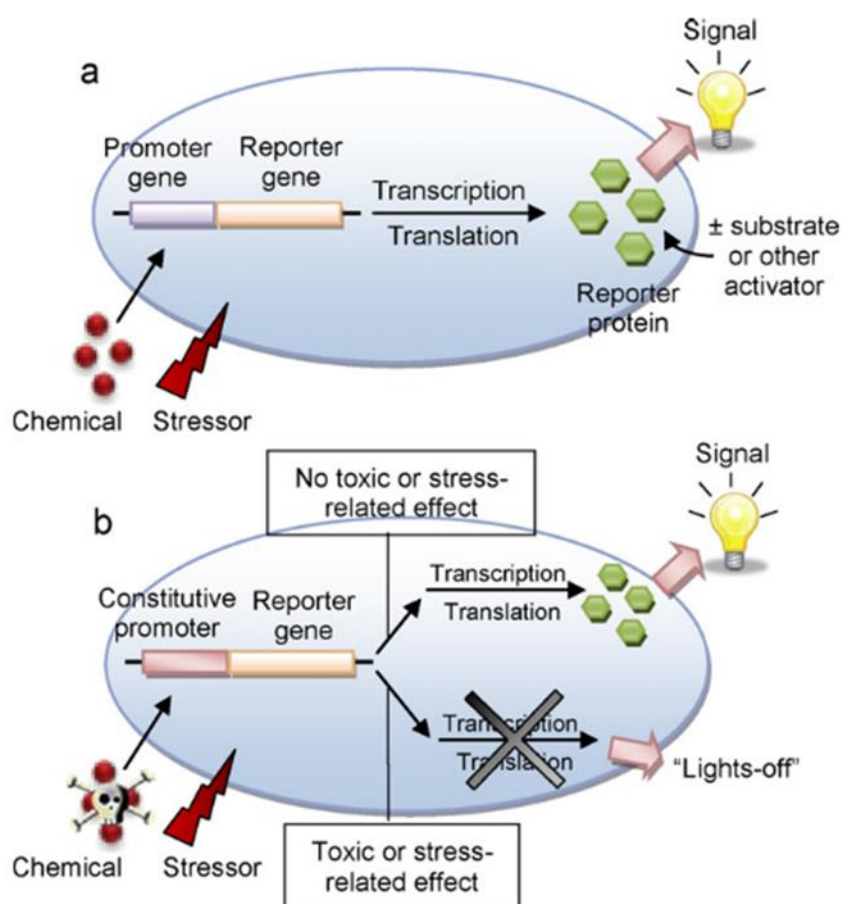


Figure 1.2 On/off switch systems of bioreporters (Xu et al., 2013)

In lights-on bioreporters, presence of chemical or stressor stimulates the expression of reporter genes. Thus, reporter protein production is correlated with the portion of the chemical/stressor. In lights-off systems, reporter gene is expressed constitutively, and presence of stressor is understood by decrease in amount of reporter protein.

1.3.2. Classification of Bioreporters

1.3.2.1. Cell Types

Based on the chemicals that will be detected and monitored, specific cell types are chosen in the design of whole cell biosensors. Bacteria-based bioreporters are the most common bioreporters that are studied to be used in environmental toxicity assays. Due to their adaptation and defense mechanisms against chemicals such as heavy metals, aromatic compounds and various toxins, bacteria cells are widely preferred in toxicity detection systems.

Recently, to be able to assess the effect and bioavailability of human related products like pharmaceuticals and hormones, there is an increasing tendency towards using eukaryotic cells as bioreporters. By being a lower eukaryote, yeast cells are valuable biomonitoring tools. Their single cell nature, ease of use and genetic manipulation techniques make them popular among research groups. Yeast cells are engineered to express the human estrogen receptor and used for detection and monitoring of estrogenic/androgenic compounds from environmental samples. In addition to yeast-based reporters, human cell-based bioreporters are developed to sense same compounds (Xu et al., 2013).

1.3.2.2. Promoters

Promoters are DNA regions that found on upstream of a gene and lead to initiation of transcription event. Great numbers of promoters are used in whole cell biosensor systems. Genes of these promoters have role in metabolism of target chemical or defense mechanism. They are stimulated in the presence of target chemical and reporter gene products are expressed as a response. The most common promoters that are used in whole cell biosensor studies are *recA* (DNA repair, SOS response), *grpE* and *ibpA* (heat shock response), *micF* (RNA stress response). In addition to stress response gene promoters, metal metabolizing gene promoters are commonly used too like *zntA*, *cadC*, *arsR* and *merR* (Van Der Meer & Belkin, 2010).

1.3.2.2.1. Heat Shock Gene Promoter, *grpE*

Heat shock response enables adaptation to cells under the stressful condition that can be physicochemical factors such as heat shock, harmful chemicals and over loading in metabolic processes. *E. coli* heat shock response includes more than 20 heat shock proteins that are responsible from expression of molecular chaperons and proteases. *grpE* gene is an example from this group and it is responsible from expression of glucose regulated protein E (Arsène, Tomoyasu, & Bukau, 2000).

grpE is a general stress responsive gene so various kinds of environmental stressors and chemicals can stimulate its expression. By using the promoter region of *grpE* gene, *E. coli* strains are used in many studies to develop whole cell biosensor for toxicity detection. *grpE* promoter is fused transcriptionally with *gfp* gene and response of cells towards environmental changes and stressors such as acid, heat and starvation is monitored (Gawande & Griffiths, 2005).

1.3.2.2.2. hdeBAD Operon Promoter

Acid stress is one of the major environmental stress of bacteria faced with in their natural habitats. Bacteria adjust their cytoplasm pH in response to acid stress but due to permeability of the outer membrane, periplasm is vulnerable to pH changes (Malki et al., 2008). Thus, enteric bacteria contain small periplasmic chaperons to protect their periplasmic protein against acid stress. *hdeA* and *hdeB* genes are the parts of acid stress operon and expressed in response to pH changes around bacteria cells. Presence of those genes are crucial for growth and survival of several enteric bacteria under low pH conditions (Dahl et al., 2015).

1.3.2.2.3. *sodA* Gene Promoter

sodA gene is responsible from expression of manganese superoxide dismutase enzyme which is responsible from destruction of reactive oxygen species (ROS) that normally produced in cells and toxic to the organisms. SoxRS transcriptional factors have direct role in activation of *sodA* promoter. Moreover, redox-cycling agents such as paraquat and chromium can induce *sodA* regulated response strongly in dose dependent manner. Therefore, *sodA* promoter fused with reporter genes and these constructs are used in paraquat monitoring assays (H. J. Lee & Gu, 2003).

1.3.2.3. Reporter Genes

While designing bioreporter cells, reporter genes are introduced to get detectable signal as evidence for the presence of chemical or stressor. Based on reporter genes, output can be colorimetric, fluorescence or bioluminescence product. Common reporter genes that are used in studies (Bereza-Malcolm, Mann, & Franks, 2015) are given in Table 1.1.

Table 1.1 Examples from commonly used reporter genes

Gene	Protein	Output
<i>bfp</i>	blue fluorescence protein	blue fluorescence
<i>crtI</i>	deinoxanthin carotenoid	pigment color change
<i>gfp</i>	green fluorescence protein	green fluorescence
<i>lacZ</i>	β -galactosidase	pH change
<i>luc</i>	firefly luciferase	bioluminescence
<i>lux</i>	bacterial luciferase	bioluminescence
<i>rfp</i>	red fluorescence protein	red fluorescence
<i>yfp</i>	yellow fluorescence protein	yellow fluorescence
<i>mtrCABF</i>	cytochrome proteins	electrons

1.3.2.4. Detection Methods

Based on selected reporter gene and output signal, different methods are used for signal detection as illustrated in Figure 1.3.

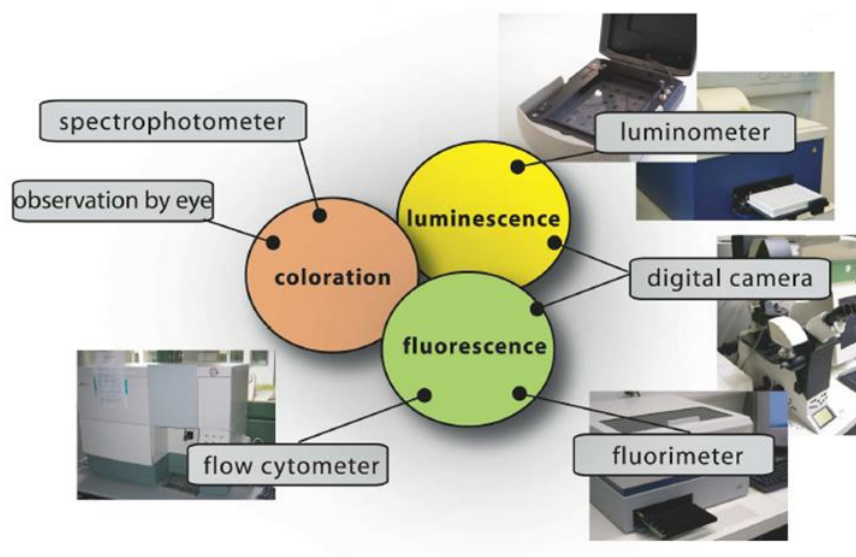


Figure 1.3 Examples for different detection methods (Tecon & van der Meer, 2008)

1.4. Aim of the Study

The aim of this study was to develop whole cell biosensor by designing new bioreporter cell constructs against boric acid, cyanide and paraquat. *E. coli* K12 MG1655 was used as a model organism and green fluorescence protein gene (gfp) was used as a reporter gene so fluorescence signal was obtained as an output. *grpE*, *hdeB* and *sodA* promoters were used in plasmid constructs to detect target chemicals.

Boric acid, cyanide and paraquat are widely used chemicals in industry and high soluble in waters. Therefore, their excessive presence in the environment has potential to have toxic effects on human health and the destruction of ecosystems. These chemicals should be tracked continuously by on-site monitoring. Therefore, instead of periodical measurements on environmental samples by chemical detection approach,

usage of whole cell biosensors is more advantageous. They are easy to perform, time saving, no need expensive equipment and highly skilled analyst. In this line, the aim of this study was developing whole cell biosensor by designing bioreporter cell against these chemicals.

CHAPTER 2

MATERIALS & METHODS

2.1. MATERIALS

2.1.1. Chemicals and Enzymes

All chemicals and enzymes used in this study were analytical grade. Induction assay chemicals H_3BO_3 and paraquat were supplied from Sigma-Aldrich, KCN was purchased from MERCK.

Taq polymerase, high-fidelity DNA polymerase Phusion® and restriction enzymes EcoRI and BamHI were supplied from Thermo Scientific and T4 DNA ligase enzyme was from New England BioLabs.

2.1.2. Media and Kits

Ingredients and preparation of media are listed in Appendix A. Distilled water was used for all preparations.

Various kits were used in this study. DNA Clean & Concentrator-5 and Zippy™ Plasmid Miniprep kits were obtained from Zymo Research and Bacterial Genomic DNA Isolation Kit was from NANObiz.

2.1.3. Buffers and Solutions

Ingredients and preparation of buffers and solutions are listed in Appendix B. Distilled water was used for all preparations.

2.1.4. Bacterial Strains, Plasmids and Primers

Two different *Escherichia coli* K-12 were used in this study. *Escherichia coli* strain DH5 α was used for cloning purposes. *Escherichia coli* strain MG1655 was used for genomic DNA extractions and polymerase chain reactions to amplify *hdeB* gene promoter. This strain was also used in transformation and planned as bioreporter organism having designed plasmids.

Escherichia coli strains were kindly provided by NANObiz Ltd. Co., Ankara, Turkey.

For molecular cloning purposes pBR322 plasmid was used. This plasmid is a double-stranded circle, 4361 bp in length and has two antibiotic resistance genes which are ampicillin resistance (AmpR) and tetracyclin resistance (TetR) genes. Transformed host cells were selected by ampicillin in the medium. Numerous restriction cut sites are present on the plasmid. In this study, EcoRI and BamHI cut sites were used for cloning purposes on pBR-sGFP plasmid.

In this study, promoterless *gfp* (encoding green fluorescence protein) gene inserted pBR322 plasmid, pBR-sGFP, was used for cloning purposes. pBR-sGFP, pBR-*grpE*-sGFP, and pBR-*sodA*-sGFP plasmids were kindly provided by Evrim Elçin (METU).

All primers were purchased from PRZ Bio Technology, Ankara, Turkey.



Figure 2.1 pBR-sGFP Map (Elcin & Öktem, 2018)

2.1.5. Instruments

Various instruments were used for different purposes in this study. Micro-volume spectrophotometer μ LITE, BioDrop was used for measurement of concentration, 260/280 and 260/230 absorbance ratios of genomic DNA sample. Microplate Spectrophotometer Multiskan™ GO, Thermo Scientific™ was used for absorbance measurements of bacteria cells to monitor cell growth. Fluorospectrometer NanoDrop™ 3300, Thermo Scientific™ was used for fluorescence measurements after induction assays. Fluid microscope EVOS FLoid Cell Imaging Station, Thermo Scientific™ was used to observe *gfp* expression in induced cells via fluorescence output.

2.2. METHODS

2.2.1. Growth Conditions of Bacteria Strains

For aseptic purposes, all culture preparations were done near the Bunsen burner flame in laminar flow hood. To prevent contamination, surface of the hood was wiped with 70% ethanol and sterilized with ultraviolet (UV) light before and after working in the hood. Equipment and liquids were autoclaved, and micropipettes were wiped with 70% ethanol before usage in the hood.

Both strains *E. coli* K-12 DH5 α and MG1655 have same growth conditions. For short term storage, cells were maintained in petri plates with LB 1.5% agar medium in 4 °C.

To grow cells, inoculation is applied into LB broth medium in flasks. Then flasks were placed in the incubator at 37 °C with 150 rpm constant shaking for 18 h.

2.2.2. Preparation of Competent Bacteria

In following steps, to be able to transform target cells with designed plasmid, firstly competent cells were prepared from both *E. coli* strains. Rubidium chloride (RbCl) competent cell protocol was followed (Green & Rogers, 2014). By this way, cell wall structures of cells were altered, and passage of foreign DNA was eased.

Two different buffer solutions named as Buffer 1 and Buffer 2 were used in this experiment. Their preparations are given in Appendix B.

At the first day, overnight culture was prepared by inoculating a colony from target strains petri plate into 5 mL LB broth. Cell growth was conducted at 37 °C with 150 rpm constant shaking in incubator for approximately 18 hours.

In the following day, 1 mL overnight culture was added to 100 mL LB medium in 250 mL flask and incubated at 37 °C with shaking at 150 rpm in incubator until the OD600 value reached 0.4 (approximately in 3.5 hours). Then, 25 mL cultures were placed into 4 x 50 mL falcon tubes and incubated on ice for 15 minutes. In the next step, falcon tubes were centrifugated at 3500 rpm at 4 °C for 10 minutes, and supernatants were discarded. Pellets are resuspended in ice-cold 2.5 mL Buffer 1 that were placed on ice. Once again, centrifugation step was applied at 3500rpm at 4 °C for 10 minutes. This time, pellets were resuspended in ice-cold 1 mL Buffer. In total, 4 mL competent cell culture was obtained, and aliquoting done as 60 µL. Finally, 2 mL tubes were frozen with liquid nitrogen and stored at -80 °C.

2.2.3. Agarose Gel Electrophoresis

For this study, agarose gel electrophoresis was applied for several steps. Volume of 1% agarose gel was adjusted in respect to sample number. To prepare 50 mL 1% gel, 0.5 g agarose is dissolved in 50 mL 1X TAE (Appendix B) and before pouring into electrophoresis gel tray 3.5 µL ethidium Bromide (5mg/ml) was added into solution.

2.2.4. Molecular Genetics Methods

2.2.4.1. Genomic DNA Isolation from *E. coli* K-12 MG1655 Cells

For bacterial genomic DNA isolation from *E. coli* K-12 MG1655 cells, overnight culture was prepared by inoculating the single colony into 5 mL LB broth (Appendix A). Cell growth was conducted at 37 °C with 150 rpm constant shaking in incubator for approximately 18 hours. NANObiz DNA4U Bacterial Genomic DNA Isolation Kit was used and the procedure was performed as stated by the manufacturer's instructions. After obtaining genomic DNA, its concentration was determined by BioDrop µLITE device, and agarose gel electrophoresis technique was applied for integrity and purity control.

2.2.4.2. Polymerase Chain Reaction (PCR) Primer Design of *hdeB* Gene Promoter from gDNA of *E. coli* K-12 MG1655 Cells

To amplify *hdeB* gene promoter (465 bp region) from genomic DNA of *E. coli* strain MG1655, one forward and one reverse primer were designed by using eurofins PCR Primer Design Web Tool (<https://www.eurofinsgenomics.eu/en/ecom/tools/pcr-primer-design/>). *hdeB* gene sequence is given in Appendix C. Primer sequences were given at Table 2.1.

Table 2.1 Primer sequences for amplification of *hdeB* gene promoter

Description	Sequence (5'-3')
pHdeB-fwd	GTTGTAGAATTCTGCTGAATAACCCGACAATAAG
pHdeB-rvs	GTGGTAGGATCCCGTAATATCCTCAACTATAAAG

200 μ M primer stocks were prepared with ultrapure, sterile and nuclease free water in stated amount according to the manufacturer's guide.

For PCR reactions, 10 μ M primer solutions were prepared from stock solution. All primer solutions were stored at -20 °C.

2.2.4.3. Amplification of Promoters

2.2.4.3.1. Gradient PCR

Gradient PCR was applied for determination of optimal annealing temperature of the primers which were designed for amplification of the promoter region of *hdeB* gene. Based on T_m temperature of primers, four points were chosen between 56 °C and 59 °C as annealing temperature.

Components, conditions and cycling program of gradient PCR are given in Tables 2.2 and 2.3.

Table 2.2 Gradient PCR reaction mixture

Components	Volume (μL)	Final concentration
dH ₂ O	8.2	-
10 X Taq buffer	2	1 X
25 mM MgCl ₂	1.5	1.88 mM
5 mM dNTP	1	0.25 mM
10 μM forward primer	1	0.5 μM
10 μM reverse primer	1	0.5 μM
gDNA of MG1655 strain	5	-
<i>Taq</i> polymerase	0.3	-
Total volume	20	-

All materials were kept on ice during preparation of the reaction mixture. After applying quick vortex and spin down to prepared PCR tubes, they were put into the assigned wells* (between 56 °C and 59 °C) of thermal cycler machine.

Table 2.3 Gradient PCR reaction condition for 465bp amplicon

Steps	Temperature (°C)	Time
Initial Denaturation	97	4 minutes
23 cycles	Denaturation	35 seconds
	Annealing	20 seconds
	Extension	30 seconds
Final Extension	72	3 minutes

To decide the best annealing temperature for the primers, agarose gel electrophoresis technique was applied. 20 μL samples were mixed with 4 μL 6 X loading dye and loaded into wells. 3 μL molecular weight marker was loaded onto the uppermost well. Finally, the gel was run at 80 V for 45 minutes.

2.2.4.3.2. Phusion (High Fidelity) PCR

By gradient PCR, Ta temperature for the primers was chosen as 57 °C. To amplify 465 bp region of *hdeB* gene promoter efficiently, high fidelity DNA polymerase enzyme Phusion® was used in this PCR reaction.

Components, conditions and cycling program of gradient PCR are given in Tables 2.4 and 2.5.

Table 2.4 Phusion PCR reaction mixture

Components	Volume (µL)	Final concentration
dH ₂ O	9.3	-
5 X HF (high-fidelity) buffer	4	1 X
5 mM dNTP	1	0.25 mM
10 µM forward primer	1	0.5 µM
10 µM reverse primer	1	0.5 µM
gDNA of MG1655 strain	3.5	-
Phusion®	0.2	-
Total volume	20	-

Table 2.5 Phusion PCR reaction condition for 465 bp amplicon

Steps	Temperature (°C)	Time
Initial Denaturation	98	1 minute
21 cycles	Denaturation	35 seconds
	Annealing	20 seconds
	Extension	15 seconds
Final Extension	72	3 minutes

2.2.4.4. Purification of PCR Products

After Phusion PCR was completed, DNA Clean & Concentrator-5 Kit of Zymo Research was used. Manufacturer's instructions were followed.

To check the quality and concentration of purified PCR products, agarose gel electrophoresis was conducted with 1% agarose gel.

2.2.4.5. pBR-sGFP Plasmid Isolation from Transformed *E. coli* K-12 DH5 α Cells

For plasmid isolation from pBR-sGFP transformed *E. coli* K-12 DH5 α cells, overnight culture was prepared by inoculating loopful cells into 5 mL LB broth (Appendix A). Cell growth was conducted at 36 °C with 150 rpm constant shaking in incubator for approximately 18 hours. ZyppyTM Plasmid Miniprep Kit of Zymo Research was used by following the manufacturer's instructions. In final step, elution was done by 35 μ L nuclease free water for 2 tubes. Thus, in total, 70 μ L pBR-sGFP plasmid was obtained. To check the quality and concentration of isolated plasmid, agarose gel electrophoresis was conducted with 1% agarose gel.

2.2.4.6. Restriction Digestion for Insert and Vector Preparation

Two restriction enzymes were used for insert and vector preparations. DoubleDigest Calculator of Thermo Scientific Web Tool (<https://www.thermofisher.com/tr/en/home/brands/thermo-scientific/molecular-biology/thermo-scientific-restriction-modifying-enzymes/restriction-enzymes-thermo-scientific/double-digest-calculator-thermo-scientific.html>) was used for determination of the ratio of enzymes and Tango Buffer volumes. 2V Tango buffer and BamH1 enzyme and 1V EcoR1 enzyme were used. Incubation temperature was recommended as 37 °C for this reaction by the Web Tool.

Reaction mixture was prepared as listed in Table 2.6. Reactions were conducted in five tubes at 37 °C for 14.5 hours.

Table 2.6 Restriction digestion reaction

Components	Plasmid (μL)	PCR product (μL)
Plasmid/ PCR product	17	17
Tango Buffer	5	5
EcoRI	2	2
BamHI	1	1
Total volume	25	25

2.2.4.7. Purification of Restriction Digestion Products

After restriction digestion reaction was completed, DNA Clean & Concentrator-5 Kit (Zymo Research) was used to purify the reaction products.

To check the quality and concentration of purified restriction digestion products, agarose gel electrophoresis was conducted with 1% agarose gel.

2.2.4.8. Ligation Reaction

According to the concentration of purified plasmid vector and insert, two ligation reaction mixtures were prepared in 1:1 and 1:3 (vector/insert) ratios as given in Table 2.7. NEBioCalculator Web Tool (<https://nebiocalculator.neb.com/#!/ligation>) was used for determination of volumes of components.

Table 2.7 Ligation reaction mixture

Components	Volume (1:1) (μL)	Volume (1:3) (μL)
Plasmid vector	10	10
Insert	2.5	7
dH ₂ O	4.5	-
Mixtures were incubated at 70 °C for 5 minutes. Then tubes were taken from thermal cycler and following components were added.		
T4 ligase buffer	2	2
T4 ligase	1	1
Total volume	20	20

Reaction mixtures were incubated at 16 °C for 19 hours for the ligation reaction to take place.

2.2.4.9. Transformation of Competent *E. coli* K-12 DH5 α Cells

465 bp region of *hdeB* promoter was cloned into pBR-sGFP plasmid vector and pBR-*hdeB*-sGFP plasmids were obtained. The next step was transformation of the competent cells with this designed plasmid. Previously prepared competent *E. coli* K-12 DH5 α cell stocks were used in this step.

Firstly, two tubes of competent *E. coli* K-12 DH5 α cell stocks were taken from -80 °C and put on ice for 5-6 minutes. There was 60 μ L of cells in tubes. 6 μ L ligation product was added into each tube and bottom of tubes was hit gently for mixing. Then tubes were placed on ice for 20-30 minutes. Water bath was adjusted to 42 °C for heat-shock step. Tubes were put on water bath for 60 seconds then taken out immediately and put into ice again for 5 minutes. Next, 950 μ L LB medium was added onto tubes and tubes were sealed with parafilm. Then, cells were incubated at 37 °C with 130 rpm for 75 minutes. After cell growth and recovery, tubes were centrifuged at 8000 g for 1 minute. 700 μ L of supernatant was discarded and cells were dissolved in remaining 300 μ L medium by gentle pipetting. 100 μ L of cell mixtures from each tube (1:1 and 1:3) were spreaded on the selective media which were 100 mg/L ampicillin containing LB agar plates. Finally, these plates were incubated at 36 °C for max 18 hours.

2.2.4.10. Colony PCR

To be able to find positive colonies, colony PCR was applied. Components, conditions of the reaction and colony PCR primer regions are given in Tables 2.8, 2.9 and 2.10.

After pinch of colonies was placed into separate PCR tubes, 17.7 μ L nuclease free water was added and tubes were vortexed. Then, tubes were placed to thermal cycler device at 98 °C for 10 minutes for bursting of colonies. Then, master mix was prepared according to the number of chosen colonies as listed in the following table. So, reaction mixture volume in each tube was completed to 25 μ L.

Table 2.8 Colony PCR reaction mixture

Components	Volume per reaction (μ L)	Final concentration
dH ₂ O	17.7	-
10 X Taq buffer	2.5	1 X
25 mM MgCl ₂	1.5	1.5 mM
5 mM dNTP	1	0.2 mM
10 μ M forward primer	1	0.4 μ M
10 μ M reverse primer	1	0.4 μ M
Taq polymerase	0.3	-
Total volume	25	-

Table 2.9 Colony PCR primer regions

Description	Sequence (5'-3')
Col-fwd	ATCACGAGGCCCTTTCGTCTTCAAGAATTC
Col-rvs	ACGCTGCCCCGAGTTATCATTATTTGTAGAGCTC

Table 2.10 Conditions of colony PCR

Steps	Temperature (°C)	Time
Initial Denaturation	98	2 minutes
27 cycles	Denaturation	95
	Annealing	57
	Extension	72
Final Extension	72	3 minutes

At the end of colony PCR reaction, assessment of colonies was done via agarose gel electrophoresis.

2.2.4.11. Plasmid Isolation from Transformed *E. coli* K-12 DH5 α Cells

Transformation of competent *E. coli* DH5 α cells with the designed pBR-*hdeB*-sGFP plasmid was proven by colony PCR.

As a first step for plasmid isolation, overnight cultures were prepared from positive colonies. They were inoculated in 100mg/L ampicillin containing 5 mL LB medium. The cultures were incubated at 36 °C with 150 rpm for 18 hours.

Next day, ZyppyTM Plasmid Miniprep Kit of Zymo Research was used by following the manufacturer's instructions. In the final step of the protocol, plasmid elution was done by 35 μ L nuclease free water.

2.2.4.12. Restriction Cut of Plasmid for Verification

After plasmid isolation, restriction cut with BamHI enzyme was applied as given in Table 2.11.

Table 2.11 Restriction cut reaction

Components	Volume (μ L)
Plasmid	18
BamHI buffer	2
BamHI enzyme	0.7
Total volume	20.7

Reaction was conducted at 37 °C for 75 minutes. Next, agarose gel electrophoresis was applied for verification of the plasmid. Plate stocks of transformed *E. coli* K-12 DH5 α cells were prepared on 120 mg/L ampicillin containing LB agar plates.

2.2.4.13. Transformation of Competent *E. coli* K-12 MG1655 Cells

Previously prepared competent *E. coli* K-12 MG1655 cell stocks were used in this step.

Firstly, two tubes of competent *E. coli* K-12 MG1655 cell stocks were taken out from -80 °C and put on ice for 5-6 minutes. 1.5 µL isolated pBR-*hdeB*-sGFP plasmid was added into each tube and gently hit on bottom of tubes for mixing. Then tubes were placed on ice for 20-30 minutes. While waiting, water bath was adjusted to 42 °C for heat-shock step. When time was up, tubes were put on water bath for 60 seconds and taken out immediately. The tubes were then put into ice again for 5 minutes. Next, 950 µL LB medium was added onto tubes and tubes were sealed with parafilm. Then, cells were incubated at 37 °C with 130 rpm for 750 minutes. After cell growth and recovery of plasma membrane, tubes were centrifugated at 8,000 xg for 1 minute. 800 µL of supernatant was discarded and cells were dissolved in remaining 200 µL medium by gentle pipetting. Cell mixtures from each tube were spreaded on the selective media which were 120 mg/L ampicillin containing LB agar plates. Finally, these plates were incubated at 37 °C for max 18 hours.

2.2.4.14. Plasmid Isolation from Transformed *E. coli* K-12 MG1655 Cells

Firstly, overnight cultures were prepared from positive colonies. They were inoculated into 100mg/L ampicillin containing 5 mL LB medium. Incubation occurred at 37 °C with 150 rpm for 18 hours.

Next day, Zyppy™ Plasmid Miniprep Kit of Zymo Research was used by following the manufacturer's instructions. In final step of the protocol, plasmid elution was applied. After plasmid isolation, restriction cut with BamHI enzyme was applied as in Table 2.11 in previous section.

2.2.5. Induction Assays

Up to this section, *E. coli* K-12 MG1655 cells were transformed with designed pBR-*hdeB*-sGFP plasmid. Two different cell constructs, which contained pBR-*grpE*-sGFP and pBR-*sodA*-sGFP plasmid separately, were kindly provided by Evrim Elçin.

First day, overnight cultures were prepared from stock plates of pBR-sGFP, pBR-*hdeB*-sGFP, pBR-*grpE*-sGFP, pBR-*grpE*-sGFP cell constructs. A single colony was inoculated into 100 mg/L ampicillin containing 10 mL M9 medium (Appendix A) in 50 mL sterile falcon tubes.

Next day, after approximately 18 hours incubations, 400 µL overnight culture cells were inoculated into 100 mg/L ampicillin containing 20 mL M9 medium in 50 mL sterile flasks. Cell growth was conducted at 37 °C with 160 rpm till OD600 values reached between 0.05 and 0.1. Then, induction chemicals were added to flask with respect to defined final concentrations, as illustrated in following three sections, and flasks were placed into the incubator again. In addition to those preparations, pBR-sGFP flask was prepared to be used as blank in RFU measurements.

2.2.5.1. H₃BO₃ (Boric Acid) Detection by *grpE* Gene Promoter

Six different concentrations were chosen to induce cells. Concentration ranges were defined according to safe limits for cell growth. Seven sterilized flasks (50 mL) were prepared for induction step, and one was used for uninduced control group.

1 M H₃BO₃ solution was prepared by usage of autoclaved dH₂O. Induction volumes are given as Table 2.12.

Table 2.12 H₃BO₃ detection by *grpE* gene promoter

Chemical	Volume	Final Concentration (mM)
1 M H ₃ BO ₃	100 μL	5
	200 μL	10
	400 μL	20
	600 μL	30
	800 μL	40
	1 mL	50

2.2.5.2. KCN (Cyanide) Detection by *hdeB* Gene Promoter

Six different concentrations were chosen to induce cells. Concentration ranges were defined according to safe limits for cell growth. Seven sterilized flasks (50 mL) were prepared for induction step, and one was used for uninduced control group.

1 mM and 10 mM KCN solutions were prepared via usage of autoclaved dH₂O. Induction volumes are given as Table 2.13.

Table 2.13 KCN (cyanide) detection by *hdeB* gene promoter

Chemical	Volume	Final Concentration (mM)
1 mM KCN	100 μL	5
	200 μL	10
	1 mL	50
10 mM KCN	200 μL	100
	400 μL	200
	600 μL	300

2.2.5.3. Paraquat Detection by *sodA* Gene Promoter

Five different concentrations were chosen to induce cells. Concentration ranges were defined according to safe limits for cell growth. Six sterilized flasks (50 mL) were prepared for induction step, one for uninduced control group.

Paraquat stocks were prepared via usage of autoclaved dH₂O. Induction volumes are given in Table 2.14.

Table 2.14 Paraquat detection by *sodA* gene promoter

Chemical	Volume	Final Concentration
100 nM Paraquat	400 μ L	2 nM
1 μ M Paraquat	{ 200 μ L	10 nM
	{ 1 mL	50 nM
100 μ M Paraquat	{ 200 μ L	1 μ M
	{ 500 μ L	2.5 μ M

2.2.5.4. Fluorescence Measurement

OD₆₀₀ and relative fluorescence unit (RFU) values were obtained at 3rd, 6th, 9th, 18th and 24th hours.

For OD₆₀₀ measurement, at predetermined time points, 1 mL sample from each flask was put into plastic cuvettes, and OD₆₀₀ measurement was done by using spectrophotometer device (Thermo Scientific™ Multiskan™ GO) at a wavelength of 600 nm. M9 medium was used as blank.

At each time point, plastic cuvettes and eppendorf tubes were prepared by addition of 1 mL samples. After getting OD₆₀₀ values, cells in eppendorf tubes were centrifugated at 10,000 xg for 2 minutes. Supernatants were discarded. Cells were resuspended in phosphate buffered saline (PBS) buffer (Appendix B). PBS volumes for each tube were calculated from OD₆₀₀ values to adjust new OD₆₀₀ values as 1. pBR-sGFP cell construct's tube was used as blank. RFU measurement was done by fluorospectrometer (Thermo Scientific™ NanoDrop™ 3300) at a wavelength of 509 nm.

2.2.5.5. Microscope Image

Fluorescence microscope images were taken at 18th and 24th hours after the inductions. Microscope slides were prepared by 5 μ L samples from same tubes which were prepared for RFU measurements. Images were taken at white channel (bright field) and blue channel (excitation: 390/40 nm, emission: 446/33 nm) by using Floid microscope (EVOS FLoid Cell Imaging Station, Thermo Scientific™).

2.2.5.6. Data Analysis

Induction experiments were performed at least three biological replicates, with three technical repeats for each biological replicate. Absorbance data at 600 nm was used to construct growth curve of induction groups. For RFU and fluorescence microscopy data, one of the three replicas from each set of experiments was presented. Percentage increases in fluorescence (RFU) for each experiment groups were calculated by using following equation and illustrated as bar graphs.

$$\% \text{ increase in RFU} = \frac{\text{RFU of induction group} - \text{RFU of control group}}{\text{RFU of control group}} \times 100$$

Equation 1 Calculation of % increase in fluorescence (RFU)

CHAPTER 3

RESULTS & DISCUSSION

3.1. Cloning Studies with *E. coli* Cells

3.1.1. Genomic DNA Isolation from *E. coli* K-12 MG1655 Cells

Concentration and purity of genomic DNA were determined by BioDrop μ LITE device, and agarose gel electrophoresis technique was applied for quality control.

Table 3.1 Purity of MG1655 gDNA

Sample	Concentration (ng/ μ L)	A260/A280	A260/A230
MG1655 gDNA	160	1.978	1.632

Purity assessments of nucleic acids and proteins can be done by measuring their absorbances at distinct wavelengths. They have maximum absorbance values at 260 and 280 nm. Ratio of these values (A260/280) gives an idea about the sample purity. Specifically, for DNA, ~1.8 is considered as optimum ratio for purity. Lower than this value means contamination of the sample by proteins and/or chemicals. Besides, absorbance at 230 nm is another sign for contamination. If 260/230 value is higher than the respective 260/280 value, nucleic acid samples are often considered as pure. Expected 260/230 values are commonly in the range of 2.0–2.2. In Table 3.1, A260/A280 value is close to optimum value for purity. However, A260/A230 value is lower than A260/A280. This means contamination of gDNA in small quantities.

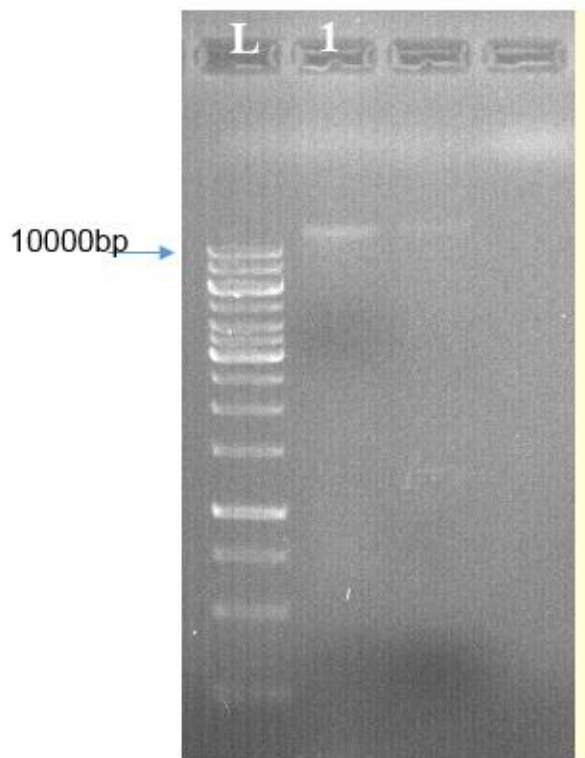


Figure 3.1 1% Agarose Gel Electrophoresis Result for *E. coli* MG1655 gDNA

L: 1 kb DNA ladder. Lane 1: *E. coli* K12 MG1655 genomic DNA

MG1655 complete genome consists of 4,639,675 bp circular DNA. Since it is in supercoiled form, runs faster than expected so observed at the above of 10 kb band in Figure 3.1.

3.1.1.1. Gradient PCR to Decide Annealing Temperature of Primers

Gradient PCR was applied to decide on the best annealing temperature of primers which were designed for the amplification of promoter region of *hdeB* gene. After completion of the reaction, agarose gel electrophoresis was conducted.

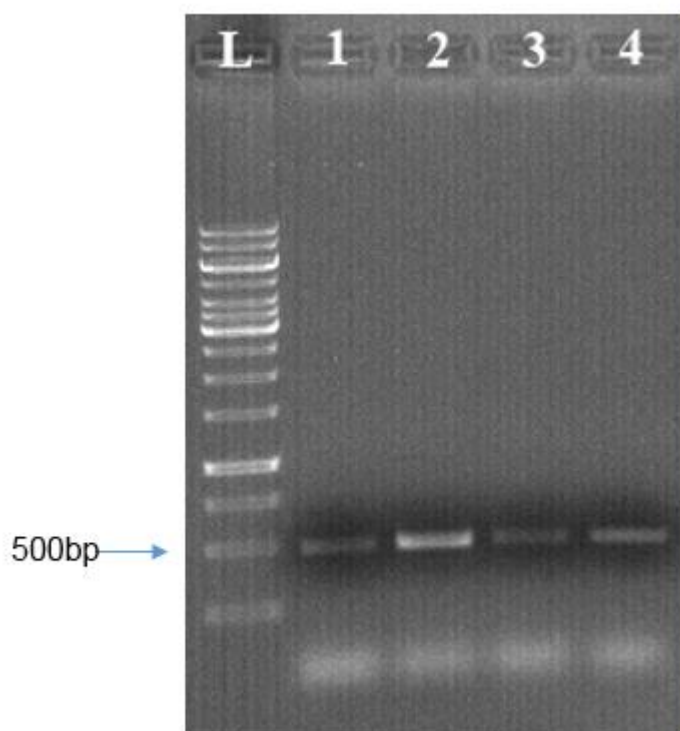


Figure 3.2 1% Agarose gel electrophoresis for PCR products.

L: 1 kb DNA ladder. Lane 1 to lane 4, each has conducted at annealing temperatures in ascending order from 56 °C to 59 °C.

As seen in the gel image (Figure 3.2), targeted region was amplified successfully at all four-annealing temperature. Since Lane 2 has the highest amplification, 57 °C was chosen as optimum annealing temperature for the next steps.

3.1.1.2. Cloning of *hdeB* Gene Promoter into pBR-sGFP Plasmid

To check the quality and concentration of purified PCR products and isolated pBR-sGFP plasmid, agarose gel electrophoresis was conducted with 1% agarose gel (Figure 3.3).

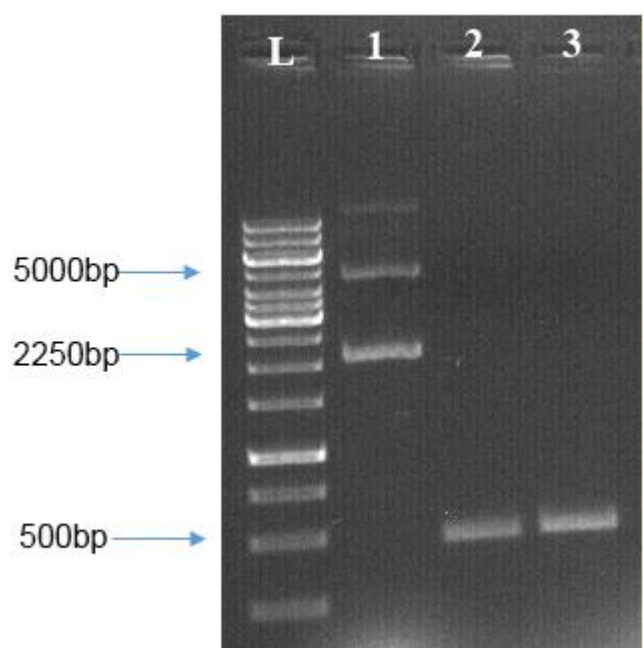


Figure 3.3 1% Agarose gel electrophoresis result for pBR-sGFP plasmid and Phusion PCR products.

L: 1 kb DNA ladder. Lane 1: Circular pBR-sGFP plasmid DNA. Lane 2 and 3: Phusion PCR products in separate reaction tubes.

Linear length of pBR-sGFP plasmid DNA is 3703 bp. However, an isolated and uncut plasmid produced two bands on the gel (Figure 3.3.) representing the supercoiled (ccc) and open circular (oc) conformations. A condensed supercoiled knot of ccc-DNA shows less friction against the agarose matrix than large, loose open circle of oc-DNA. Hence, for the same over-all size, supercoiled DNA runs faster than open-circular DNA. So, in Lane 1, two bands were observed. One was oc form at approximately 5000 bp, other was ccc form in between 2000 bp and 2500 bp. If the plasmid is cut

once with a restriction enzyme, however, the supercoiled and open-circular conformations are all reduced to a linear conformation. Thus, one band would be observed at 3700 bp line.

Targeted region on genomic DNA was 465 bp and with the addition of restriction enzyme cut region and random nucleotide region via primers, final amplicon length went up 489 bp. Therefore, Phusion PCR product were observed at approximately 500 bp line as expected.

3.1.2. Restriction Digestion for Insert and Vector Preparation and Purification

For insert and vector preparation, restriction digestion reaction was conducted by using EcoRI and BamHI enzymes. In the following step, reaction products were purified via DNA Clean & Concentrator-5 Kit of Zymo Research. To check the quality and concentration of purified restriction digestion products, agarose gel electrophoresis was applied with 1% agarose gel as seen in Figure 3.4.

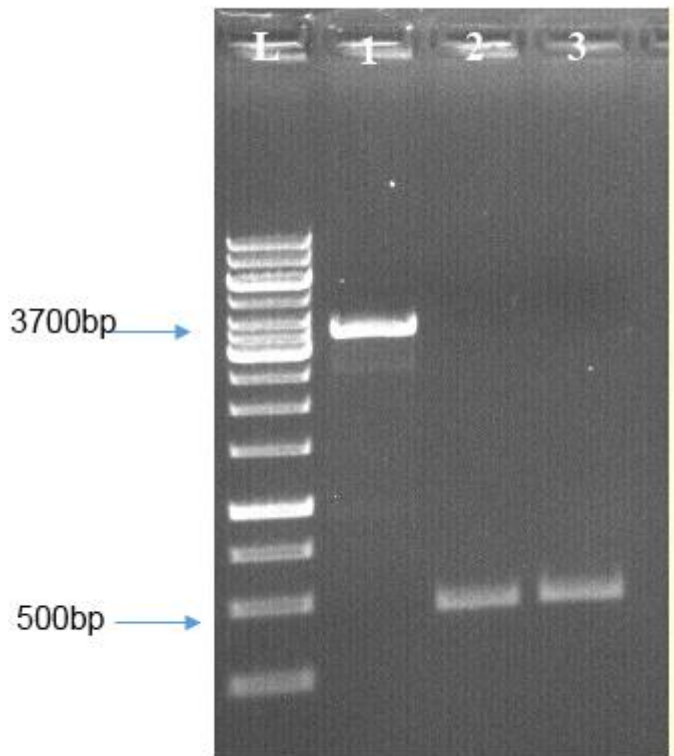


Figure 3.4 1% Agarose gel electrophoresis result for purified restriction digestion products.

L: 1 kb DNA ladder. Lane 1: Linear pBR-sGFP plasmid DNA as vector. Lane 2 and 3: 465 bp amplicon as insert.

pBR-sGFP plasmid length was 3703 bp. After restriction digestion reaction, 35 bp region was discarded from the plasmid and linear structure form was obtained. Thus, vector product was observed in between 3500 bp and 4000 bp line. Moreover, other restriction digestion product, the insert, was observed at approximately 500 bp line as expected. After that ligation reaction was conducted and transformation of competent cells was applied.

3.1.3. Colony PCR from Transformed *E. coli* K-12 DH5 α Cells

After the transformation, colony PCR was performed to find positive colonies. Several colonies were chosen and tested for the presence of pBR-*hdeB*-sGFP plasmid. Colony PCR primers amplified the region from beginning of the insert to the end of GFP gene. So, expected amplicon from colony PCR was 1215 bp (465 bp insert + 750 bp GFP gene).

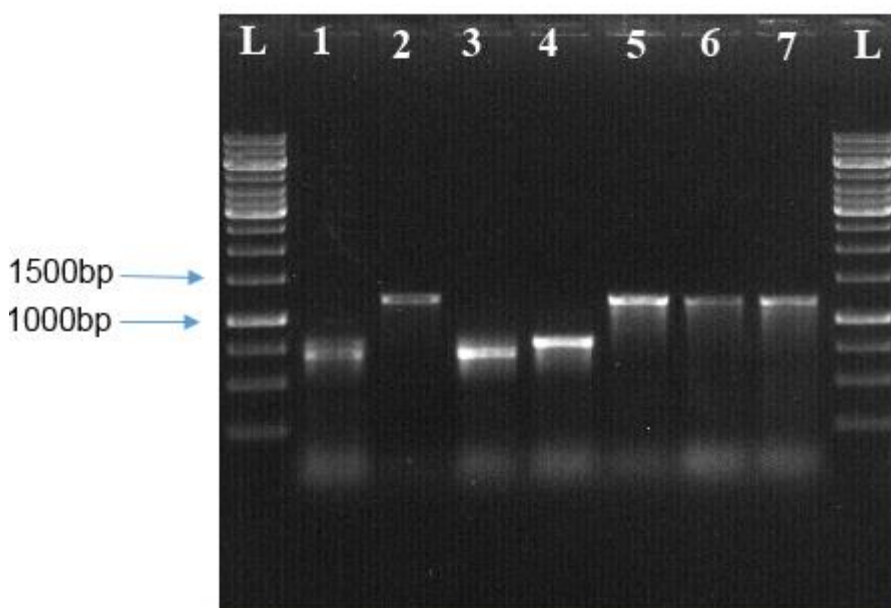


Figure 3.5 1% Agarose gel electrophoresis result for colony PCR products.

L: 1 kb DNA ladder. Lane 1 to 7: chosen colonies tested for presence of pBR-*hdeB*-sGFP plasmid.

For positive colonies, expected amplicon length was 1215 bp. In this line, colony 2, 5, 6 and 7 were positive as seen in the Figure 3.5.

3.1.4. Conformation of Ligation

Three of the positive colonies (5-7) were chosen for this step. After plasmid isolations, restriction enzyme BamHI was used for conformation. pBR-sGFP plasmid length was 3703 bp. After cutting off 35 bp region by restriction digestion and inserting *hdeB* gene promoter, pBR-*hdeB*-sGFP plasmid length was expected in approximately 4200 bp lane and obtained as seen in Figure 3.6.

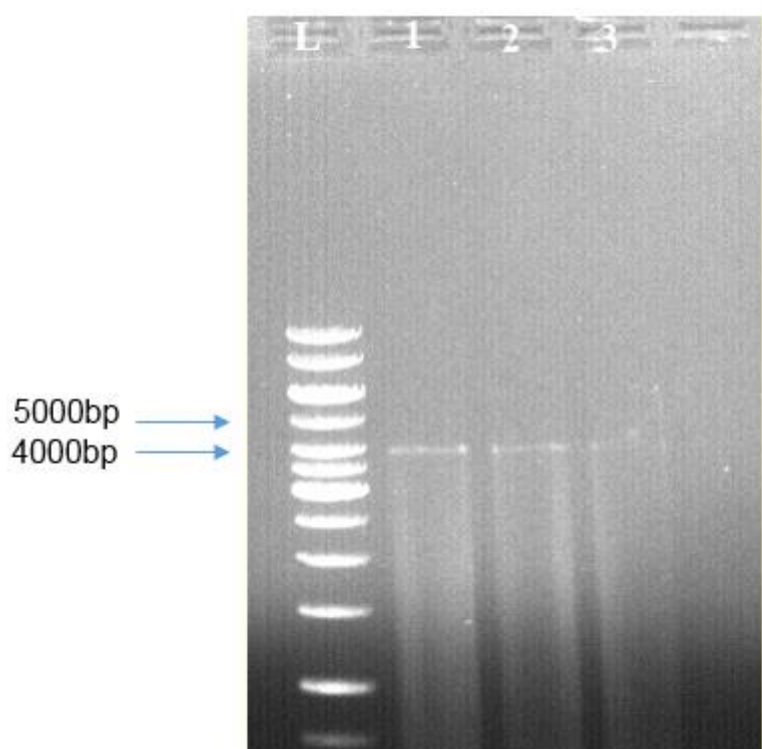


Figure 3.6 1% Agarose gel electrophoresis result for conformation of ligation.

L: 1 kb DNA ladder. Lane 1 to 3: Conformation of positive colonies (5-7) via BamHI cut.

All three colonies were observed at the expected line. Since Lane 1 was the shiniest, therefore following step continued with colony 5.

All colonies were expected to contain pBR-*hdeB*-sGFP plasmid. Three of them were chosen for conformation. After overnight culture preparation and 18 hours cell growth,

plasmid isolation step was applied. Then, restriction enzyme BamHI was used for conformation. By cutting plasmids from one point, length of linear form was checked. As seen in Figure 3.7. all plasmids were observed at the expected length.

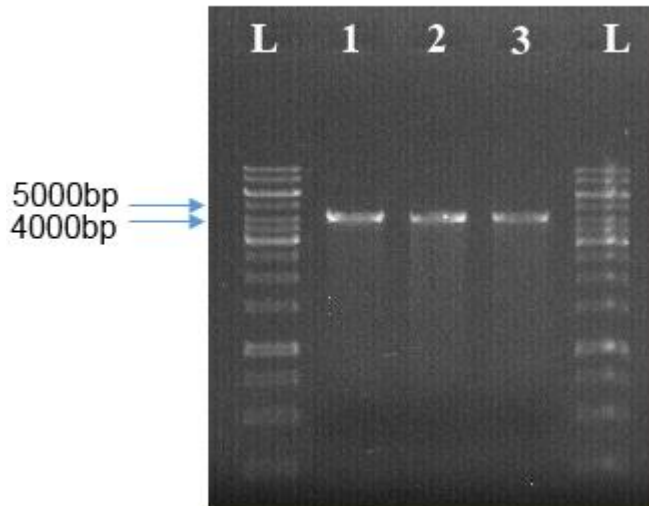


Figure 3.7 1% Agarose gel electrophoresis result for conformation of *E. coli* K-12 MG1655 cells transformation.

L: 1 kb DNA ladder. Lane 1 to 3: Conformation of positive colonies via BamHI cut.

All three MG1655 colonies were positive for the presence of pBR-*hdeB*-sGFP plasmid. One of them was streaked into a 100 mg/L ampicillin containing LB agar plate and those cells were used in the induction assays.

So far, pBR-*hdeB*-sGFP plasmid containing *E. coli* MG1655 cells were prepared. Other two construct, pBR-*grpE*-sGFP and pBR-*sodA*-sGFP were provided. All constructs were ready for the induction assays.

3.2. Induction Assays

3.2.1. H₃BO₃ Detection

Growth assessment of samples that were treated with boric acid at different concentrations was done by absorbance measurement at 600 nm. Time points for growth curve were chosen as 3rd, 6th, 9th, 18th, and 24th hours. Absorbance values are given in Table 3.2 and the growth curve given in Figure 3.8.

Table 3.2 Absorbance values of pBR322 and seven pBR-*grpE*-sGFP induction groups at distinct time points

Absorbance Result of Boric Acid Induction at Distinct Time Points								
(h)	pBR322	0	5 mM	10 mM	20 mM	30 mM	40 mM	50 mM
3 rd	0.64±0.03	0.65±0.02	0.58±0.01	0.53±0.01	0.40±0.02	0.36±0.06	0.32±0.01	0.29±0.01
6 th	1.16±0.07	1.18±0.09	1.15±0.02	1.02±0.06	0.85±0.06	0.76±0.01	0.73±0	0.51±0.01
9 th	1.14±0.02	1.37±0.03	1.41±0.03	1.23±0.05	1.13±0.02	1.06±0.04	1.02±0.04	0.57±0.08
18 th	2.07±0.06	2.04±0.03	2.04±0.06	1.86±0.08	1.76±0.03	1.69±0.03	1.72±0.07	0.63±0.01
24 th	2.05±0.06	2.05±0.01	2.06±0.03	1.92±0.02	1.77±0.02	1.69±0.01	1.91±0.02	0.84±0.05

As observed at Figure 3.8, till 40 mM boric acid concentration, induction groups showed same growth pattern with negative control. The group treated with 50 mM boric acid had lower cell growth. This shows that 50 mM and higher concentrations have negative effect on cell growth. Minimum inhibitory and bactericidal concentration of boric acid on a different *E. coli* strain was determined as 7.60 mg/mL (approximately 120 mM) (Yilmaz, 2012). In this line, since decent cell growth was desired, upper boric acid concentration was chosen as 50 mM for this experiment.

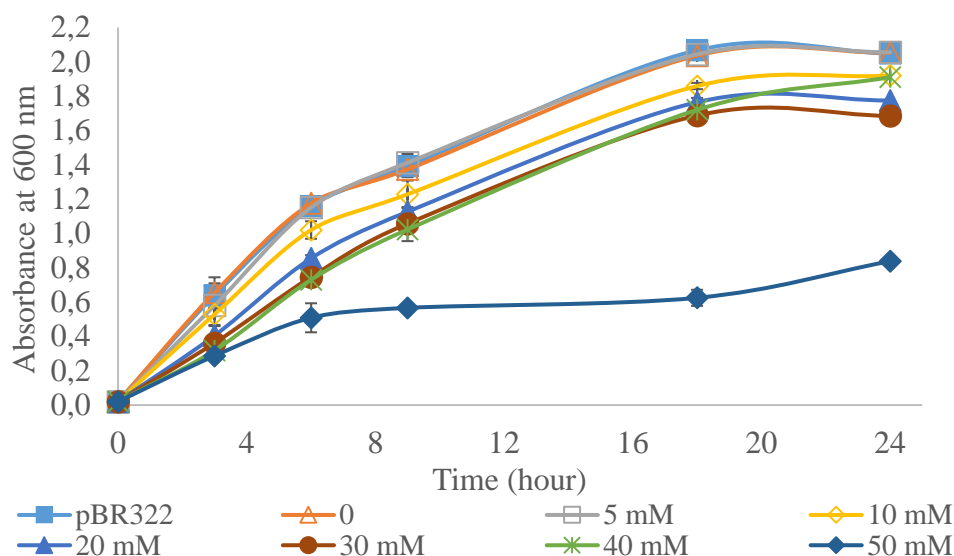


Figure 3.8 Growth curves of pBR322 and boric acid treated seven pBR-*grpE*-sGFP induction groups at distinct time points

At each time point, after OD measurement, RFU values were obtained to track the response of cells by GFP production towards boric acid. Fluorescence measurements were done at 509 nm wavelength (gfp excitation at 488 nm, emission at 509 nm). As an illustration of the measurement screen, RFU result of 40mM boric acid treated group from 9th hour is given at Appendix D. RFU values are given at Table 3.3.

Table 3.3 RFU values of boric acid treated seven pBR-*grpE*-sGFP induction groups at distinct time points

RFU Values at Different Induction Concentrations							
Hour	0	5 mM	10 mM	20 mM	30 mM	40 mM	50 mM
3 rd	34.2±2.0	38.5±0.8	47.8±1.6	42.3±1.6	53.2±1.8	32.9±3.4	25.6±1.8
6 th	36.9±1.4	44.0±1.9	61.5±2.8	77.7±2.1	79.6±4.1	91.4±3.0	83.2±3.1
9 th	62.5±3.0	64.6±1.8	83.5±2.1	106.7±2.7	114.1±3.6	135.3±1.8	122.2±7.1
18 th	27.1±1.9	32.7±3.2	51.6±3.0	73.7±3.8	82.3±1.9	107.9±3.3	138.5±4.5
24 th	33.5±2.5	38.8±1.3	57.2±1.6	79.2±1.2	92.5±1.0	115.3±4.9	103.9±1.7

5 mM boric acid treated group had similar fluorescence value with control group so boric acid in this concentration does not have significant effect on *gfp* expression.

When results of control and induction groups in Figure 3.9 are compared, the most remarkable increase in fluorescence amount was observed at 18th hour. While 40 mM boric acid treatment caused 300% increase in fluorescence, 50 mM boric acid treated cells showed over %400 increase. According to literature search done by during this study, there was no study about boric acid detection via whole cell biosensor approach with *grpE* gene promoter. Thus, by this construct, pBR-*grpE*-sGFP, boric acid detection can be applied in between 40 mM and 50 mM concentrations.

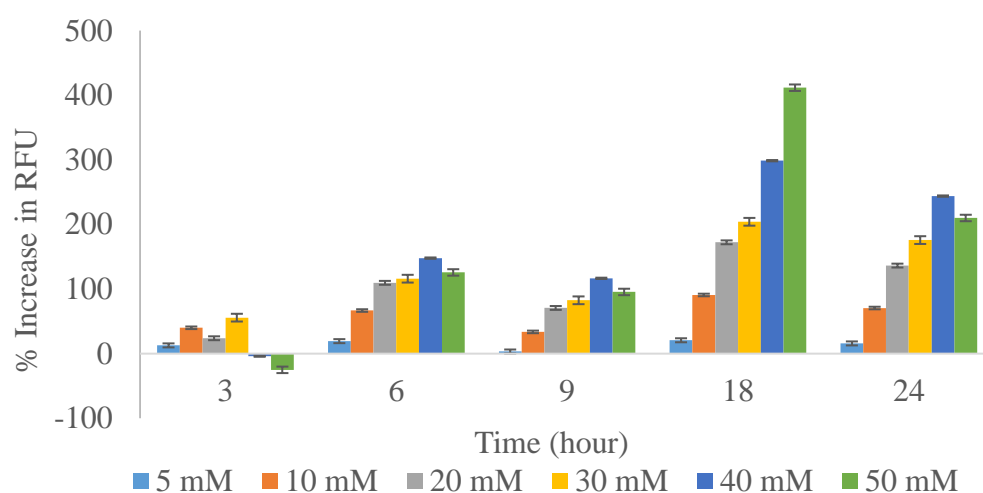


Figure 3.9 % increase of fluorescence (RFU) for six boric acid treated groups in comparison with control group at distinct time points.

At 3rd hour, 40 mM and 50 mM boric acid treated groups showed less fluorescence expression than control group. These concentrations might be high for the first phase of the cell growth. After that, cells showed adaptation to these concentrations and higher fluorescence expression against boric acid.

Figure 3.10 illustrates fluorescence microscope images of control group and 50 mM boric acid treated induction group at 18th hour. Induced cell group (on the right) was brighter in comparison with the control group (on the left) due to higher *gfp* expression which was in agreement with RFU data (Table 3.3).

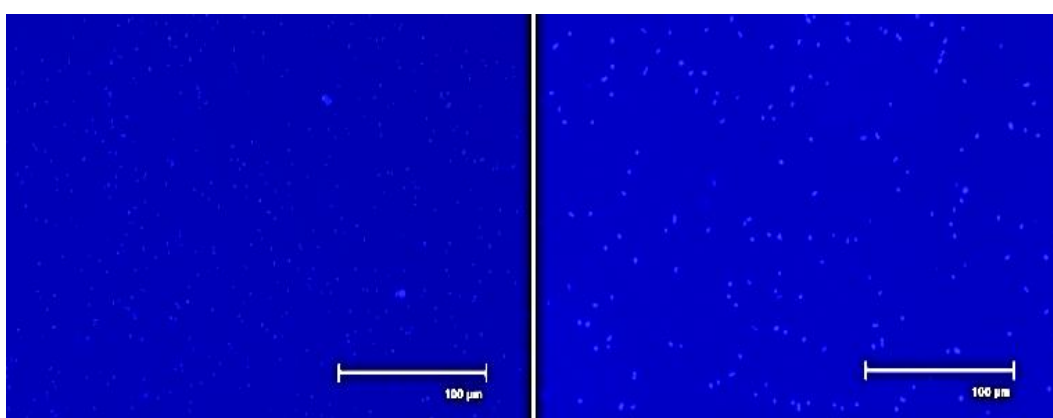


Figure 3.10 Fluorescence microscope images of control group and 50 mM H_3BO_3 treated induction group at 18th hour

White, bright dots on blue background represents cells. Since detection limit determined as 50 mM at 18th hour for boric acid, fluorescence microscope image of this group was chosen.

3.2.2. KCN (Cyanide) Detection

Growth assessment of samples that were treated with KCN at different concentration was done by absorbance measurement at 600 nm. Time points for growth curve were chosen as 3rd, 6th, 9th, 18th, and 24th hours. Absorbance values are given in Table 3.4 and the growth curve given in Figure 3.11.

Table 3.4 Absorbance values of pBR322 and seven pBR-*hdeB*-sGFP induction groups at distinct time points

Absorbance Result of Cyanide Induction at Distinct Time Points								
(h)	pBR322	0	5 μ M	10 μ M	50 μ M	100 μ M	200 μ M	300 μ M
3 rd	0.64 \pm 0.03	0.58 \pm 0.03	0.53 \pm 0.02	0.49 \pm 0.01	0.17 \pm 0.01	0.12 \pm 0.01	0.09 \pm 0.01	0.09 \pm 0
6 th	1.14 \pm 0.03	1.15 \pm 0.02	1.03 \pm 0.05	0.98 \pm 0.01	0.22 \pm 0.01	0.31 \pm 0.03	0.11 \pm 0.01	0.10 \pm 0
9 th	1.40 \pm 0.02	1.41 \pm 0.01	1.29 \pm 0.10	1.12 \pm 0.03	0.98 \pm 0.02	0.93 \pm 0.09	0.51 \pm 0.02	0.46 \pm 0.03
18 th	2.02 \pm 0.07	2.06 \pm 0.06	1.86 \pm 0.07	1.60 \pm 0.11	1.52 \pm 0.06	1.29 \pm 0.09	0.91 \pm 0.02	0.84 \pm 0.04
24 th	1.99 \pm 0.07	1.98 \pm 0.01	1.82 \pm 0.06	1.76 \pm 0.12	1.60 \pm 0.04	1.44 \pm 0.12	1.24 \pm 0.06	0.89 \pm 0.04

As observed at Table 3.4 and Figure 3.11, while pBR-sGFP and control group showed same growth pattern, decreased cell growth was observed at induction groups in proportion to KCN concentration. Since higher concentration of cyanide has negative effect on cell growth.

Effect on potassium cyanide on respiratory system of *E. coli* was studied with different carbon sources. Thus, according to chosen carbon source for bacteria cells, toxic concentration of potassium cyanide varied in between 250 μ M and 1 mM (Knowles, 1976). In this study, glucose was the carbon source for the cells so upper limit for potassium cyanide concentration was determined as 300 μ M.

5 μM cyanide treated group showed similar growth pattern with control group. This concentration of cyanide might not have any effect on cell growth

From 50 μM to 300 μM cyanide treated cells showed slow cell growth till 6th hour and tried to adapt presence of cyanide around. Then after a small peak, showed slow growth pattern again. Especially 200 μM and 300 μM cyanide treated cells seemed to have toxic effect of high concentration of cyanide.

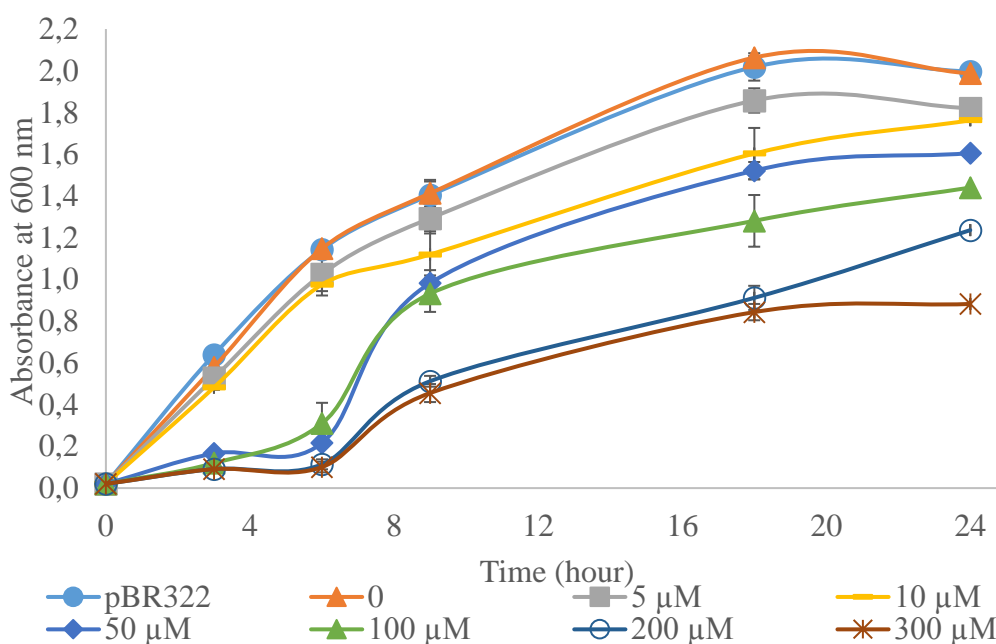


Figure 3.11 Growth curves of pBR322 and cyanide treated seven pBR-*hdeB*-sGFP induction groups at distinct time points

At each time point, after OD measurement, RFU values were obtained to track response of cells by GFP production towards presence of KCN. Fluorescence measurements were done at 509 nm wavelength. As an illustration of measurement screen, RFU result of 100 μM KCN treated group from 9th hour is given at Appendix D. RFU values are given in Table 3.5.

Table 3.5 RFU values of potassium cyanide treated seven pBR-*hdeB*-sGFP induction groups at distinct time points

Hour	RFU Values at Different Induction Concentrations						
	0	5 μ M	10 μ M	50 μ M	100 μ M	200 μ M	300 μ M
3 rd	27.8 \pm 1.3	28.3 \pm 1.1	33.6 \pm 1.4	42.9 \pm 4.4	142.9 \pm 27.1	22.5 \pm 6.54	19.2 \pm 2.5
6 th	34.4 \pm 2.3	34.9 \pm 2.7	43.3 \pm 2.9	50.9 \pm 4.2	107.0 \pm 10.5	33.4 \pm 1.7	26.1 \pm 2.5
9 th	46.8 \pm 1.5	53.7 \pm 4.0	54.1 \pm 1.4	82.7 \pm 5.0	144.9 \pm 12.9	46.5 \pm 2.3	32.7 \pm 3.0
18 th	100.1 \pm 2.4	95.6 \pm 5.4	92.5 \pm 4.2	93.0 \pm 5.3	196.1 \pm 7.0	111.7 \pm 4.2	60.8 \pm 7.2
24 th	141.5 \pm 3.9	132.7 \pm 6.7	130.8 \pm 2.3	120.5 \pm 3.2	202.4 \pm 16.1	132.1 \pm 3.9	64.5 \pm 8.9

When results of control and induction groups are compared in Figure 3.12, the most remarkable increase in fluorescence was observed at 3rd hour. 100 μ M KCN treated cells showed over %400 increase in fluorescence. According to literature search done during this study, *hdeBAD* operon promoter was not used before in whole cell biosensor approach and for cyanide detection. Thus, by this construct, pBR-*hdeB*-sGFP, cyanide detection can be applied in around 100 μ M cyanide concentration.

200 μ M and 300 μ M potassium cyanide treated induction groups showed less fluorescence production than control group (except 18th h four 200 μ M cyanide treated group) as give in Figure 3.12. This might be caused by stress on respiratory system of bacteria cells caused by high concentration of cyanide. Because of that, expression events of cells might be halted so less *gfp* expression than control group was observed.

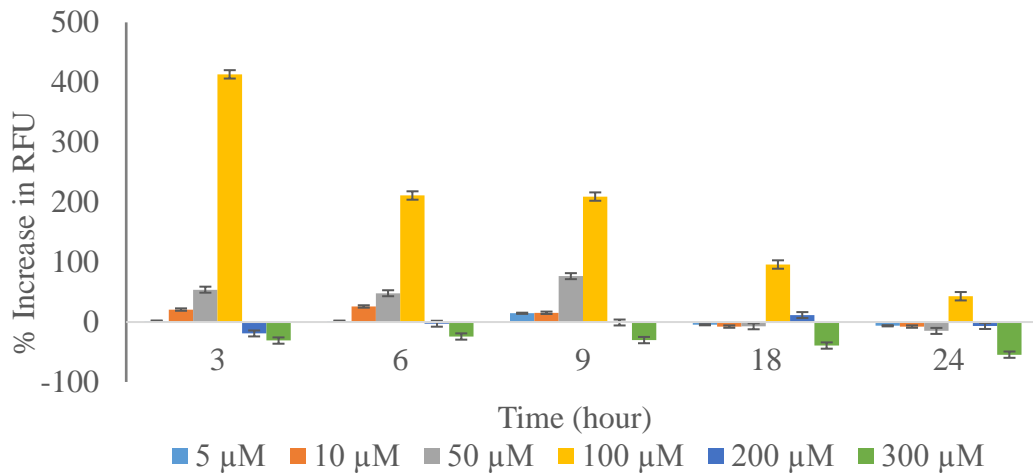


Figure 3.12 % increase of fluorescence (RFU) for six cyanide treated groups in comparison with control group at distinct time points

Figure 3.13 illustrates the fluorescence microscope images of control group and 100 μM KCN treated induction group at 3rd hour. Induced cell group (on the right) was brighter in comparison with the control group (on the left) due to higher *gfp* expression which was in agreement with RFU data (Table 3.5).

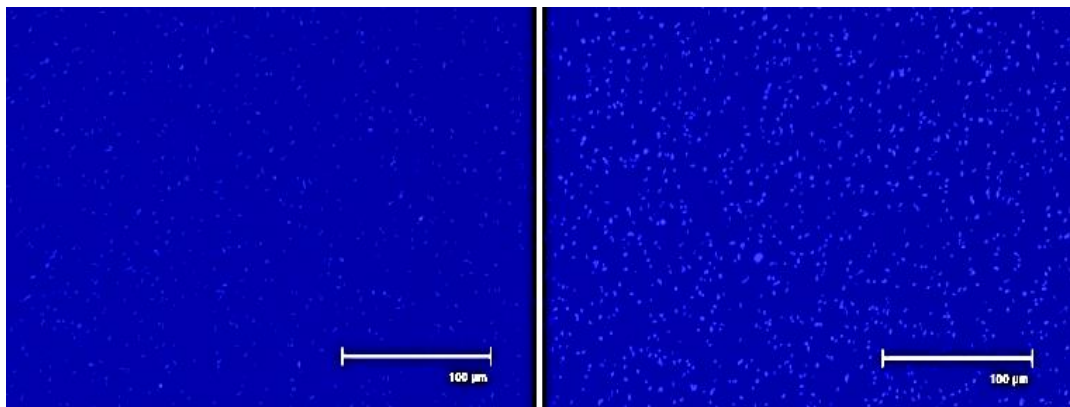


Figure 3.13 Fluorescence microscope images of control group and 100 μM KCN treated induction group at 3rd hour

White, bright dots on blue background represents cells. Since detection limit was determined as 100 μM at 3rd hour for cyanide, fluorescence microscope image of this group was chosen.

3.2.3. Paraquat Detection

Growth assessment of samples that treated with paraquat at different concentration was done by absorbance measurement at 600 nm. Time points for growth curve were chosen as 3rd, 6th, 9th, 18th, and 24th hours. Absorbance values are given in Table 3.6 and the growth curve given in Figure 3.14.

Table 3.6 Absorbance values of pBR322 and six pBR-*sodA*-sGFP induction groups at distinct time points

Absorbance Result of Paraquat Induction at Distinct Time Points							
(h)	pBR322	0	2 nM	10 nM	50 nM	1 μ M	2,5 μ M
3 rd	0.38 \pm 0	0.38 \pm 0.06	0.37 \pm 0.03	0.38 \pm 0.04	0.38 \pm 0.03	0.33 \pm 0.01	0.29 \pm 0.03
6 th	1.13 \pm 0.01	1.11 \pm 0.06	1.14 \pm 0.09	1.13 \pm 0.07	1.06 \pm 0.04	1.02 \pm 0.05	0.93 \pm 0.02
9 th	1.38 \pm 0.01	1.37 \pm 0.08	1.31 \pm 0.04	1.35 \pm 0.03	1.27 \pm 0.03	1.26 \pm 0.02	1.28 \pm 0.06
18 th	1.82 \pm 0.02	1.52 \pm 0.05	1.51 \pm 0.04	1.51 \pm 0.03	1.59 \pm 0.01	1.64 \pm 0.03	1.42 \pm 0.02
24 th	1.89 \pm 0.01	1.61 \pm 0.01	1.49 \pm 0.02	1.54 \pm 0.02	1.61 \pm 0.02	1.65 \pm 0.03	1.51 \pm 0.02

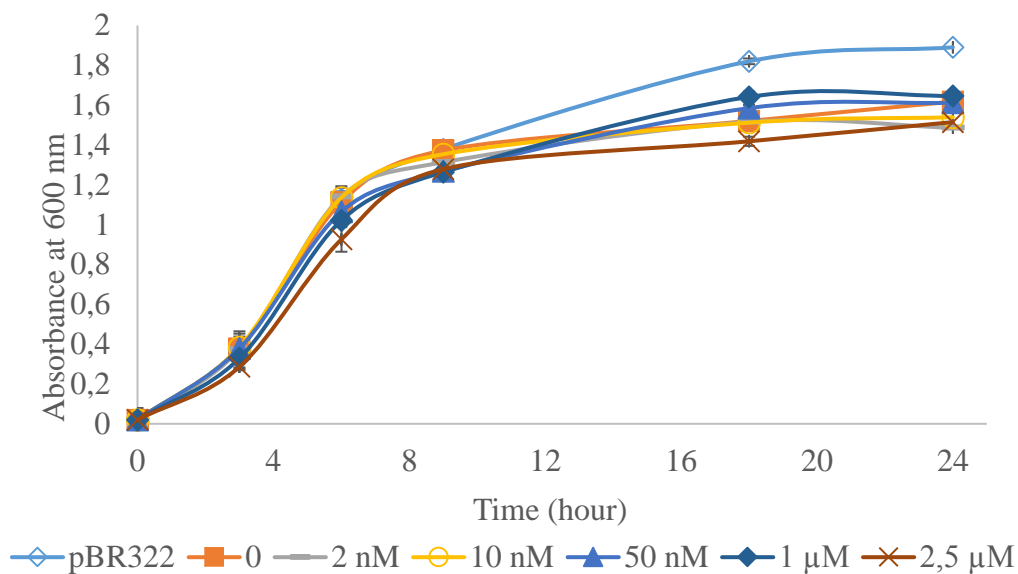


Figure 3.14 Growth curves of pBR322 and paraquat treated six pBR-*sodA*-sGFP induction groups at distinct time points

As observed as Table 3.6 and Figure 3. 14, all groups show similar growth pattern. This might be caused by the testing low concentrations of paraquat for detection, so potential toxic effect of paraquat on bacteria cell was not observed.

At each time point, after OD measurement, RFU values were obtained to track the response of cells by GFP production towards presence of paraquat. Fluorescence measurements were done at 509 nm wavelength. As an illustration of measurement screen, RFU result of 2.5 μM paraquat treated group from 9th hour is given at Appendix D. RFU values are given in Table 3.7.

Table 3.7 RFU values of paraquat treated six pBR-*grpE*-sGFP induction groups at distinct time points

Hour	RFU Values at Different Induction Concentrations					
	0	2 nM	10 nM	50 nM	1 μ M	2,5 μ M
3 rd	87.9 \pm 3.1	91.1 \pm 1.2	144.0 \pm 7.4	170.5 \pm 16.0	415.3 \pm 27,2	1116.9 \pm 93.2
6 th	47.7 \pm 4.7	46.6 \pm 2.8	80.2 \pm 2.5	97.9 \pm 5.0	258.8 \pm 82,1	684.0 \pm 33.2
9 th	59.2 \pm 6.0	59.3 \pm 9.1	75.6 \pm 2.0	123.1 \pm 34.1	178.1 \pm 46,8	533.6 \pm 32.3
18 th	28.2 \pm 3.0	33.4 \pm 2.1	49.5 \pm 11.2	190.3 \pm 2.1	204.5 \pm 7,5	156.3 \pm 3.8
24 th	26.9 \pm 1.0	24.4 \pm 2.5	65.8 \pm 13.4	239.7 \pm 22.9	203.4 \pm 3.6	140.4 \pm 2.5

When the results of control and induction groups are compared (Figure 3.15), the most remarkable increase in fluorescence amount was observed between 3rd and 9th hours. Induced cell groups showed a dose-dependent *gfp* expression to a superoxide anion generator, paraquat. Especially at 6th hour, 2,5 μ M paraquat treated group showed over 1300% increase in fluorescence (in comparison to control group). Detection limit was determined as 50 nM at 18th hour based on more than 500% increase in fluorescence.

According to literature search, *sodA* promoter is extensively used in whole cell biosensor approach and for paraquat detection. In similar studies which is done with different plasmid construct, 20 μ M and 200 μ M paraquat concentrations are tested (Lu, Bentley, & Rao, 2004). In this study, concentration range was determined between 2 nM and 2 μ M. Remarkable results are observed in lower concentrations.

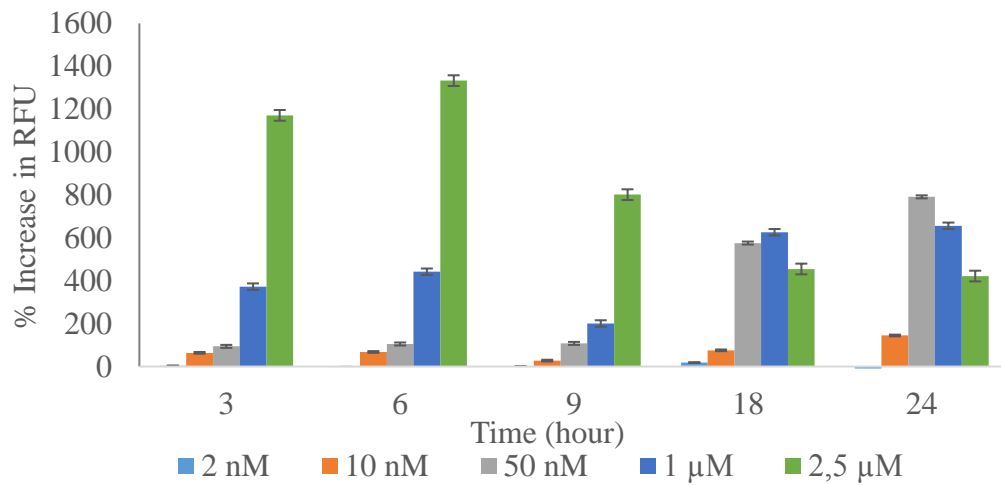


Figure 3.15 % increase of fluorescence (RFU) for five paraquat treated groups in comparison with control group at distinct time points

Figure 3.16 illustrates the fluorescence microscope images of control group and 1 μM paraquat treated induction group at 18th hour. Induced cell group (on the right) was brighter in comparison with control group (on the left) due to higher *gfp* expression which was in agreement with RFU data (Table 3.7).

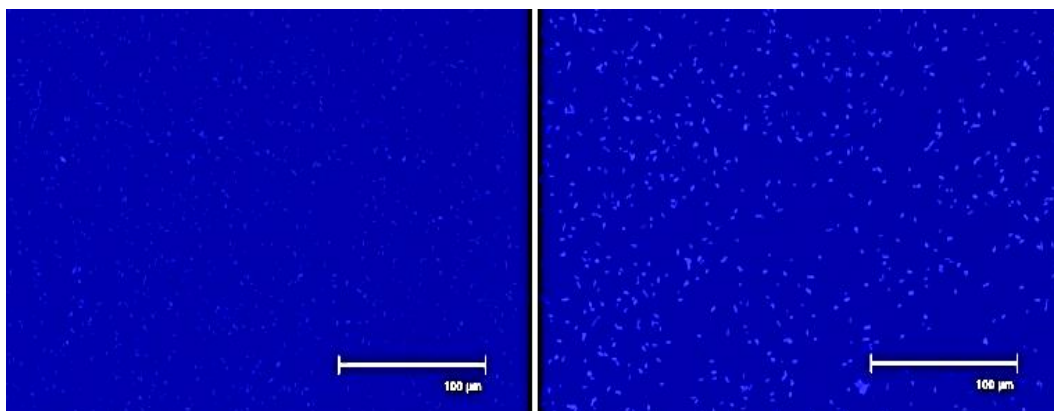


Figure 3.16 Fluorescence microscope images of control group and induced group with 1 μM paraquat at 18th hour

White, bright dots on blue background represents cells. Since detection limit was determined as 50 nM at 18th hour for paraquat, fluorescence microscope image of this group was chosen.

CHAPTER 4

CONCLUSION

The aim of this study was developing whole cell biosensor method. It is a promising method for toxicity detection in various samples such as air, soil, water and body fluids. Whole cell-based test systems offer better estimate of the real toxicology potential of the sample. They are easy to perform, time saving, no need expensive equipment and highly skilled analyst.

In this study, three different bioreporter cell constructs were designed to detect chemicals which are boric acid, cyanide and paraquat. *E. coli* K12 MG1655 cells were selected as model organisms. Green fluorescent protein was the reporter protein in this study, so fluorescence was obtained as output. *grpE*, *sodA* and *hdeBAD* operon promoters were cloned into pBR-sGFP plasmid individually and three different plasmid constructs were designed. *grpE* and *sodA* promoters are commonly used in bioreporter studies for toxicity detection. However, *grpE* constructs were not used in detection of boric acid before. Moreover, *hdeBAD* operon promoter was not included bioreporter studies at all and used for cyanide detection by using potassium cyanide as target chemical. *sodA* promoter was used for paraquat detection and lower detection limit was tested in comparison with literature.

At the end of this study, boric acid determination by pBR-*grpE*-sGFP construct, cyanide determination by pBR-*hdeB*-sGFP construct and paraquat determination by pBR-*sodA*-sGFP were tested. At least 400% increase in fluorescence signal was obtained in the experimental groups compared to the control group for detection of all three chemicals. Detection limit for boric acid decided as 50 mM, for cyanide as 100 μ M, and for paraquat as 50 nM.

These bioreporter constructs can be developed further for environmental applications. According to ongoing studies, bioreporter cells can be immobilized in solid mediums and placed into the biosensor devices. By continuous water flow, target chemical detection can be enabled in the future.

REFERENCES

- Aguilera-Sáez, L. M., Belmonte-Sánchez, J. R., Romero-González, R., Martínez Vidal, J. L., Arrebola, F. J., Garrido Frenich, A., & Fernández, I. (2018). Pushing the frontiers: Boron-11 NMR as a method for quantitative boron analysis and its application to determine boric acid in commercial biocides. *Analyst*, *143*(19), 4707–4714. <https://doi.org/10.1039/c8an00505b>
- Arsène, F., Tomoyasu, T., & Bukau, B. (2000). The heat shock response of *Escherichia coli*. *International Journal of Food Microbiology*, *55*(1–3), 3–9. [https://doi.org/10.1016/S0168-1605\(00\)00206-3](https://doi.org/10.1016/S0168-1605(00)00206-3)
- Bereza-Malcolm, L. T., Mann, G., & Franks, A. E. (2015). Environmental Sensing of Heavy Metals Through Whole Cell Microbial Biosensors: A Synthetic Biology Approach. *ACS Synthetic Biology*, *4*(5), 535–546. <https://doi.org/10.1021/sb500286r>
- Carvalho, F. P. (2017). Pesticides, environment, and food safety. *Food and Energy Security*, *6*(2), 48–60. <https://doi.org/10.1002/fes3.108>
- Chuntib, P., & Jakmune, J. (2015). Talanta Simple flow injection colorimetric system for determination of paraquat in natural water. *Talanta*, *144*, 432–438. <https://doi.org/10.1016/j.talanta.2015.06.066>
- Dahl, J., Koldewey, P., Salmon, L., Horowitz, S., Bardwell, J. C. A., & Jakob, U. (2015). HdeB Functions as an Acid-protective Chaperone in Bacteria. *Journal of Bacteriology*, *190*(1), 65–75. <https://doi.org/10.1074/jbc.M114.612986>
- Dinis-oliveira, R. (2008). Paraquat Poisonings: Mechanisms of Lung Toxicity, Clinical Features, and Critical Reviews in Toxicology, (February). <https://doi.org/10.1080/10408440701669959>
- Dong, Z., Yang, C., Vellaisamy, K., Li, G., Leung, C., Ma, D., ... Leung, C. (2017). Construction of a nano biosensor for cyanide anion detection and its application in environmental and biological systems. <https://doi.org/10.1021/acssensors.7b00553>
- Elcin, E., & Öktem, H. A. (2018). Whole-cell fluorescent bacterial bioreporter for arsenic detection in water. *International Journal of Environmental Science and Technology*. <https://doi.org/10.1007/s13762-018-2077-0>
- Gawande, P. V., & Griffiths, M. W. (2005). Effects of environmental stresses on the activities of the *uspA*, *grpE* and *rpoS* promoters of *Escherichia coli* O157:H7. *International Journal of Food Microbiology*, *99*, 91–98. <https://doi.org/10.1016/j.ijfoodmicro.2004.06.012>

- Green, R., & Rogers, E. J. (2014). Chemical Transformation of *E. coli* Rachel. *Methods*, 3–6. <https://doi.org/10.1016/B978-0-12-418687-3.00028-8>. Chemical
- Hamilton, R. A., & Wolf, B. C. (2007). Accidental boric acid poisoning following the ingestion of household pesticide. *Journal of Forensic Sciences*, 52(3), 706–708. <https://doi.org/10.1111/j.1556-4029.2007.00420.x>
- Jethava, D., Gupta, P., Kothari, S., Rijhwani, P., & Kumar, A. (2014). Acute cyanide Intoxication: A rare case of survival. *Indian Journal of Anaesthesia*, 58(3), 312. <https://doi.org/10.4103/0019-5049.135045>
- Knowles, C. J. (1976). Microorganisms and cyanide. *Bacteriological Reviews*, 40(3), 652–680.
- Konduracka, E. (2019). A link between environmental pollution and civilization disorders : a mini review.
- Lee, H. J., & Gu, M. B. (2003). Construction of a *sodA::luxCDABE* fusion Escherichia coli: Comparison with a *katG* fusion strain through their responses to oxidative stresses. *Applied Microbiology and Biotechnology*, 60(5), 577–580. <https://doi.org/10.1007/s00253-002-1168-4>
- Lee, J. H., Youn, C. H., Kim, B. C., & Gu, M. B. (2007). An oxidative stress-specific bacterial cell array chip for toxicity analysis. *Biosensors and Bioelectronics*, 22(9–10), 2223–2229. <https://doi.org/10.1016/j.bios.2006.10.038>
- Lien, C., Unnikrishnan, B., Harroun, S. G., Wang, C., & Chang, J. (2018). Biosensors and Bioelectronics Visual detection of cyanide ions by membrane-based nanozyme assay. *Biosensors and Bioelectronic*, 102(August 2017), 510–517. <https://doi.org/10.1016/j.bios.2017.11.063>
- Lu, C., Bentley, W. E., & Rao, G. (2004). A high-throughput approach to promoter study using green fluorescent protein. *Biotechnology Progress*, 20(6), 1634–1640. <https://doi.org/10.1021/bp0497511>
- Malki, A., Le, H. T., Milles, S., Kern, R., Caldas, T., Abdallah, J., & Richarme, G. (2008). Solubilization of protein aggregates by the acid stress chaperones HdeA and HdeB. *Journal of Biological Chemistry*, 283(20), 13679–13687. <https://doi.org/10.1074/jbc.M800869200>
- Moloudizargari, M., Moradkhani, F., Asghari, N., Fallah, M., Asghari, M. H., Moghadamnia, A. A., & Abdollahi, M. (2019). NLRP inflammasome as a key role player in the pathogenesis of environmental toxicants. *Life Sciences*, 231, 116585. <https://doi.org/10.1016/j.lfs.2019.116585>
- Nasir, T., Herzog, G., Hebrant, M., Despas, C., Liu, L., & Walcarius, A. (2018). Mesoporous silica thin films for improved electrochemical detection of paraquat Mesoporous Silica Thin Films for Improved Electrochemical Detection of Paraquat. <https://doi.org/10.1021/acssensors.7b00920>

- Parezanović, G. Š., Lalic-Popovic, M., Golocorbin-Kon, S., Vasovic, V., Milijašević, B., Al-Salami, H., & Mikov, M. (2019). Environmental Transformation of Pharmaceutical Formulations: A Scientific Review. *Archives of Environmental Contamination and Toxicology*, 77(2), 155–161. <https://doi.org/10.1007/s00244-019-00630-z>
- Princz, J., Becker, L., Scheffczyk, A., Stephenson, G., Scroggins, R., Moser, T., & Römbke, J. (2017). Ecotoxicity of boric acid in standard laboratory tests with plants and soil organisms. *Ecotoxicology*, (i), 1–10. <https://doi.org/10.1007/s10646-017-1789-0>
- Promchat, A., Rashatasakhon, P., & Sukwattanasinitt, M. (2017). A novel indolium salt as a highly sensitive and selective fluorescent sensor for cyanide detection in water. *Journal of Hazardous Materials*, 329, 255–261. <https://doi.org/10.1016/j.jhazmat.2017.01.024>
- Richardson, J. R., Fitsanakis, V., Westerink, R. H. S., & Kanthasamy, A. G. (2019). Neurotoxicity of pesticides. *Acta Neuropathologica*, (0123456789). <https://doi.org/10.1007/s00401-019-02033-9>
- Schoderboeck, L., Mühlegger, S., Losert, A., Gausterer, C., & Hornek, R. (2011). Chemosphere Effects assessment : Boron compounds in the aquatic environment. *Chemosphere*, 82(3), 483–487. <https://doi.org/10.1016/j.chemosphere.2010.10.031>
- Sharma, M., Akhter, Y., & Chatterjee, S. (2019). A review on remediation of cyanide containing industrial wastes using biological systems with special reference to enzymatic degradation. *World Journal of Microbiology and Biotechnology*, 35(5). <https://doi.org/10.1007/s11274-019-2643-8>
- Taylor, P., & Bolt, H. M. (n.d.). *Journal of Toxicology and Environmental Health , Part A : Current Issues Human Environmental and Occupational Exposures to Boric Acid : Reconciliation with Experimental Reproductive Toxicity Data*, (October 2014), 37–41. <https://doi.org/10.1080/15287394.2012.675301>
- Tecon, Robin; van der Meer, J. R. (2008). Bacterial Biosensors for Measuring Availability of Environmental Pollutants, 4062–4080. <https://doi.org/10.3390/s8074062>
- Van Der Meer, J. R., & Belkin, S. (2010). Where microbiology meets microengineering: Design and applications of reporter bacteria. *Nature Reviews Microbiology*, 8(7), 511–522. <https://doi.org/10.1038/nrmicro2392>
- Wasito, H., Fatoni, A., Hermawan, D., & Sutji, S. (2019). Ecotoxicology and Environmental Safety Immobilized bacterial biosensor for rapid and effective monitoring of acute toxicity in water. *Ecotoxicology and Environmental Safety*, 170(November 2018), 205–209. <https://doi.org/10.1016/j.ecoenv.2018.11.141>

- Xu, T., Close, D. M., Sayler, G. S., & Ripp, S. (2013). Genetically modified whole-cell bioreporters for environmental assessment. *Ecological Indicators*, 28, 125–141. <https://doi.org/10.1016/j.ecolind.2012.01.020>
- Yilmaz, M. T. (2012). Minimum inhibitory and minimum bactericidal concentrations of boron compounds against several bacterial strains. *Turkish Journal of Medical Sciences*, 42(SUPPL.2), 1423–1429. <https://doi.org/10.3906/sag-1205-83>
- Zhai, J., Yong, D., Li, J., & Dong, S. (2013). A novel colorimetric biosensor for monitoring and detecting acute toxicity in water. *Analyst*, 138(2), 702–707. <https://doi.org/10.1039/c2an36160d>
- Zhang, G., Qiao, Y., Xu, T., Zhang, C., Zhang, Y., Shi, L., ... Dong, C. (2015). Highly selective and sensitive nanoprobe for cyanide based on gold nanoclusters with red fluorescence emission. *Nanoscale*, 7(29), 12666–12672. <https://doi.org/10.1039/c5nr03033a>

APPENDIX A

BACTERIAL GROWTH MEDIA

Luria-Bertani (LB) Broth

10 g tryptone, 5 g yeast extract and 10 g NaCl were dissolved in 1 L of dH₂O and pH was adjusted to 7.0. Sterilization was performed by autoclaving at 121 °C for 20 minutes.

Luria-Bertani (LB) Agar (1.5%)

10 g tryptone, 5 g yeast extract, 10 g NaCl and 10 g agar were dissolved in 1 L of dH₂O and pH was adjusted to 7.0. Sterilization was performed by autoclaving at 121 °C for 20 minutes.

M9 Medium

100 mL M9 Salts (5X)(Appendix B), 10 mL 20% glucose, 1 mL 1M MgSO₄, 50 µL 1M CaCl₂, 5 mL 10% casamino acid were added into a glass bottle and volume was completed to 500 mL by sterilized dH₂O. (This recipe is for MG1655 strain. For DH5α, 50 µL 0.5% thiamine is added to mixture too.)

APPENDIX B

BUFFERS AND SOLUTIONS

1X PBS Buffer

4 g NaCl, 0.1 g KCl, 0.72 g Na₂HPO₄ and 0.12 g KH₂PO₄ were suspended in 500 mL of dH₂O. pH was adjusted to 7.4. The sterilization was done by autoclaving at 121 °C for 20 minutes.

50X TAE

242 g tris base, 57 mL acetic acid and 100 mL 0.5M EDTA were dissolved in 1 L of dH₂O. The buffer was diluted to 1 X for agarose gel electrophoresis experiments.

Buffer 1 (for competent cell preparation)

0.074 g CH₃COOK, 0.3 g RbCl, 0.37 g CaCl₂·2H₂O and 7.5 g or 3 mL glycerol were dissolved in 25mL sterilized dH₂O. It was filtered with 0.22 um syringe filter.

Buffer 2 (for competent cell preparation)

0.053 g MOPS, 0.03 g RbCl, 0.3 g CaCl₂·2H₂O and 7.5 g or 3 mL glycerol were dissolved in 25mL sterilized dH₂O. It was filtered with 0.22 um syringe filter.

M9 Salts (5X)

15 g Na₂HPO₄, 7.5g KH₂PO₄, 1,25 g NaCl and 2.5 g NH₄Cl were dissolved in 500 mL dH₂O. The sterilization was done by autoclaving at 121 °C for 20 minutes.

APPENDIX C

hdeBAD OPERON DNA SEQUENCE

CAGCACTTTTTAAACATTAAACCTGACTACGGAAAATATCAGCCATGATAATGTTTGAATGGCTAATTT
GCCATAGAGTGAAAAAATTAGATGAAATTCAGTAGGTTGAAATAATCACTAGCAGGTAATTTTCAAT
GATAGTGCGCAATTGATCTACAACACTGCGTAGCGGAGAGAGTATTAATCGGATCATAGTCACATCAAGT
GACTATGATCCGGGTGACAACCGGGGTAATTATTGCTGCTTAACGAACAACTGGCGAAGCTGAACAGGC
TGGCGGCGCTAAATATCAGTTCATCCACCAGTGTGAAAACCAGCGTTACAGACACCATCGGCGTTGC
ACCAAGGAATATCCAGGCAATGACGATATCCAGCACACCAATAACGAGCTGTAGCCAGCTGCCTTTTCATT
GAACGCTGACGATACCAACTCATCAGGCGAATAACCCCTGCAACACAGAACAAACCGGCAATAAATGCCG
CAATGGCAAAAATGCCAGCTCCGGTGCGGGATGAAGAAATAGCCGATCAATAAATAGGCGACTGCGAC
GAGAAAACCGGATAAATACCGGCCAGAAAATATGACTGCGGT TGCTGAATAACCCGACAATAAGCGCAATA
CCCGAGCAGATTAATAATGCACCCACTACTGTGCTTAAAAATATCGCCAGAGACGAACGGGAAACTGATAC
ACAGCAACCCGACGATAAACAGCAGCACGGCAATAAACTGGATTGCTCTGCGATGTTTTTAAGCATCTC
CAGATCAAACCTTCAAAATTGTTGCCTTATCTATATATAACATAGAACCACCTATAAAAATTAAGAAGAAA
ATCCCCTGCATCAATCTATGCCAAAAACGCGTCTAAGAATGCAGTCGATTTAATAAAAAATTTCTAATT
GCAGTATCTGATGCATCTGTAACCTATTGTATTGAAATAAAAAATATCTGATTTTGATATTTCCATCAAC
A TATACAGAAAACCGGT CTAAGT TCGAAATTGATTGCTGACGGCTCTTCACTTTAT
AGTTGAGGATATTACG ATG AAAAAAGTATTAGGCGTTATTCTTGGTGGTCTGCTTCTTCTGCCAGTTGTG
AGCAATGCAGCGGATGCGCAAAAAGCAGCTGATAACAAAAACCGGTCAACTCCTGGACCTGTGAAGATT
TCCTGGCTGTGGACGAATCCTTCCAGCCAACTGCAGTTGGTTTTGCTGAAGCGCTGAACAACAAAGATAA
ACCAGAAGATGCGGTTTTAGATGTTCCAGGTATTGCAACCGTAACCCCGACTATCGTTCAGGCTTGTACT
CAGGATAAACAAAGCCAACTTAAAGATAAAGTTAAAGGCGAATGGGACAAAATTAAGAAAGATATGTAAT
TCCGGAATGCGTTACATCGTACTTCCCTTGATATTGAACAGGCCGGAATATCTTCTTTAAAAGCAGCTA
TTCTCCTGTTCATATATAATCTCTATATTGAATGGTTACAAAATGAATATTTATCTCTCCGTAAAGC
GTTTTTTTTATGGGCGCTGTAGCGGCTTTGTCACTGGTGAACGCACAATCTGCGTTGGCAGCCAATGAA
TCCGCTAAAGATATGACCTGCCAGGAATTTATTGATCTGAATCCAAAAGCAATGACCCCGGTTGCATGGT
GGATGCTGCATGAAGAAACAGTATATAAAGGTGGCGATAACCGTTACTTTAAATGAAACCGATCTCACTCA
AATTCTAAAGTGATCGAATACTGTAAGAAAAACCGCAGAAAAATTTGTATACCTTCAAAAATCAAGCA
TCTAATGACTTGCCGAATTAATGAGGTGCAAGTAAAAAGGAGTAGCAAGTTGAGCCATCTTGTGCTCCT
TTTTGCATTTTTATATGACAGCAGAATTTATTATACGTCTTATACTCGCGGCAATTGCCTGTGGCGCTAT
TGGCATGGAAGGCAAAATGCGCGGCAAAGGAGCAGGGTTACGCACACATGTATTAATTGGCATGGGAAGC
GCCCTGTTTATGATTGTTTCGAAATATGGTTTTGCTGACGTGCTGTCTTTAGATCACGTCGGACTCGACC

Figure A.1 Amplified region of hdeBAD operon promoter

APPENDIX D

EXAMPLES FOR RFU RESULTS OF INDUCTION GROUPS

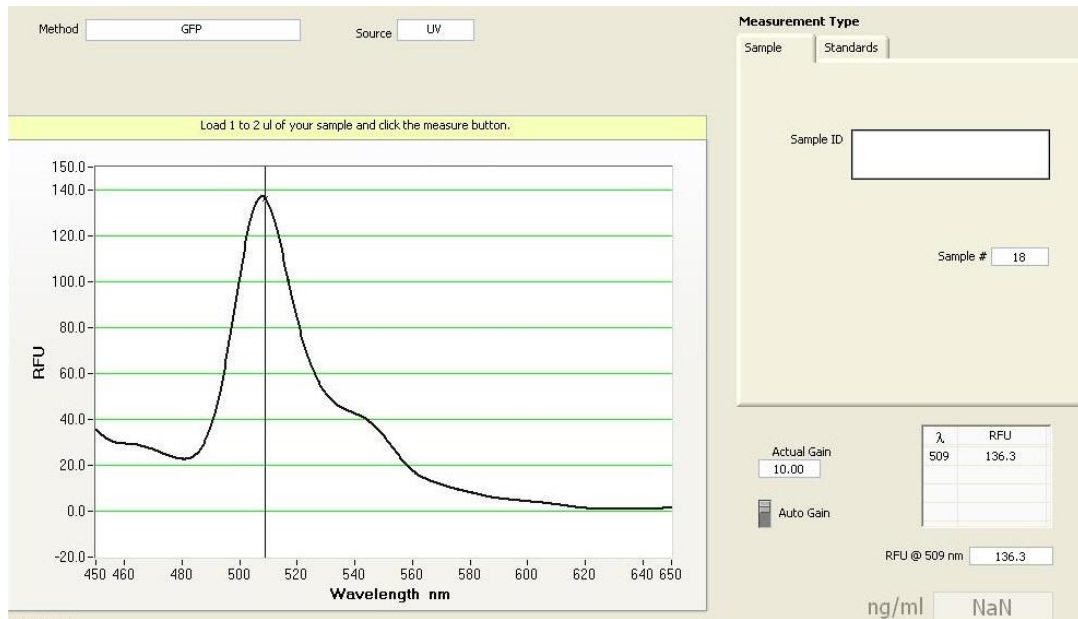


Figure A.2 RFU value of 40 mM H₃BO₃ induced sample at 9th hour

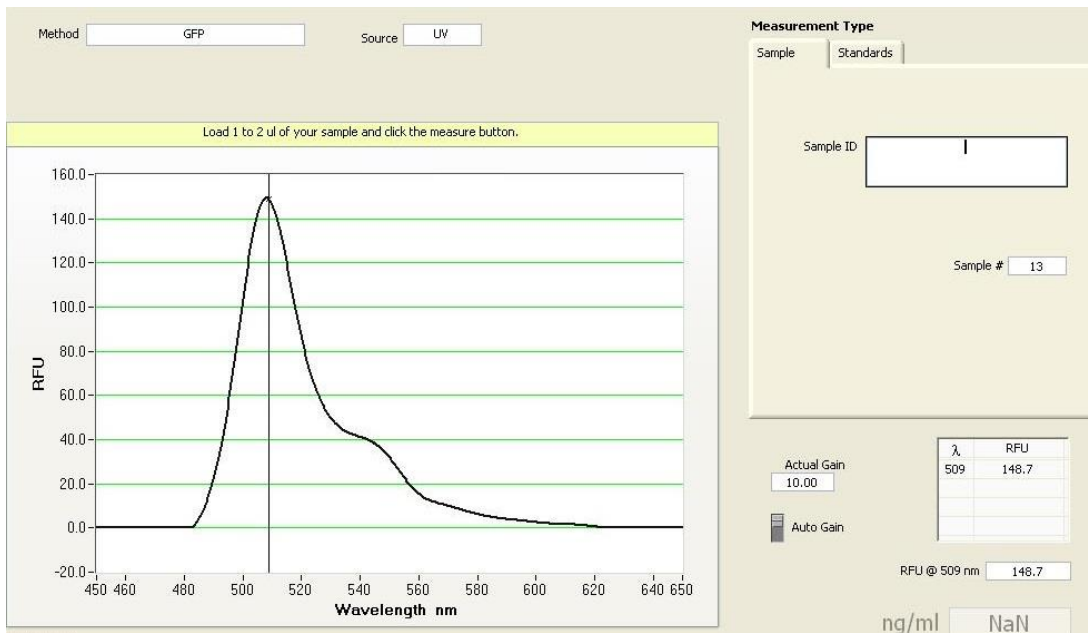


Figure A.3 RFU value of 100 μ M KCN induced group at 9th hour

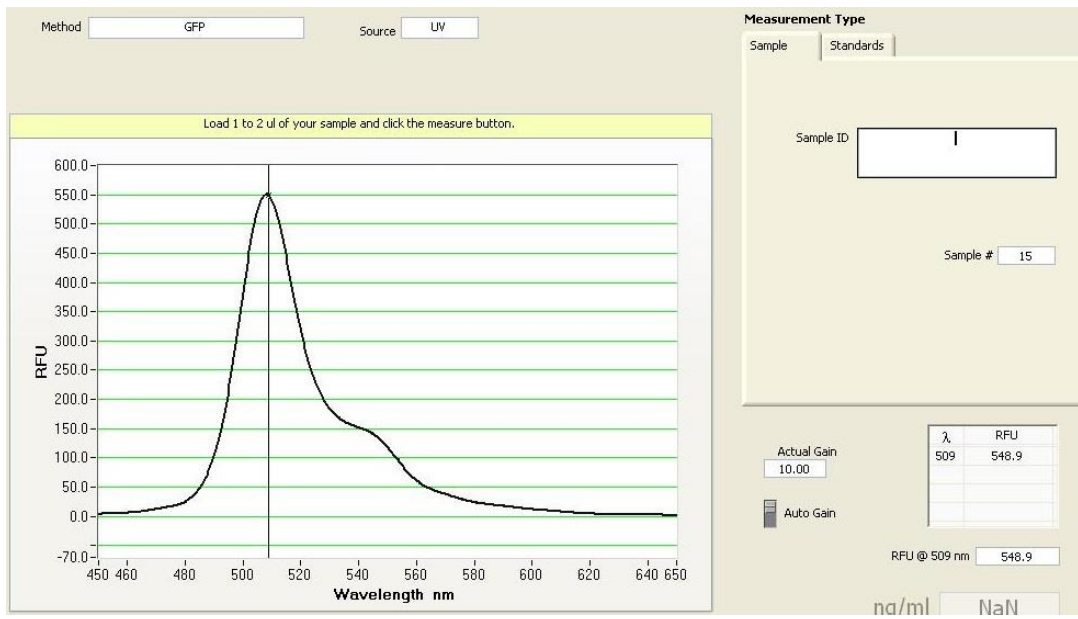


Figure A.4 RFU value of 2.5 μ M paraquat induced group at 9th hour